

PhD Preliminary Exam

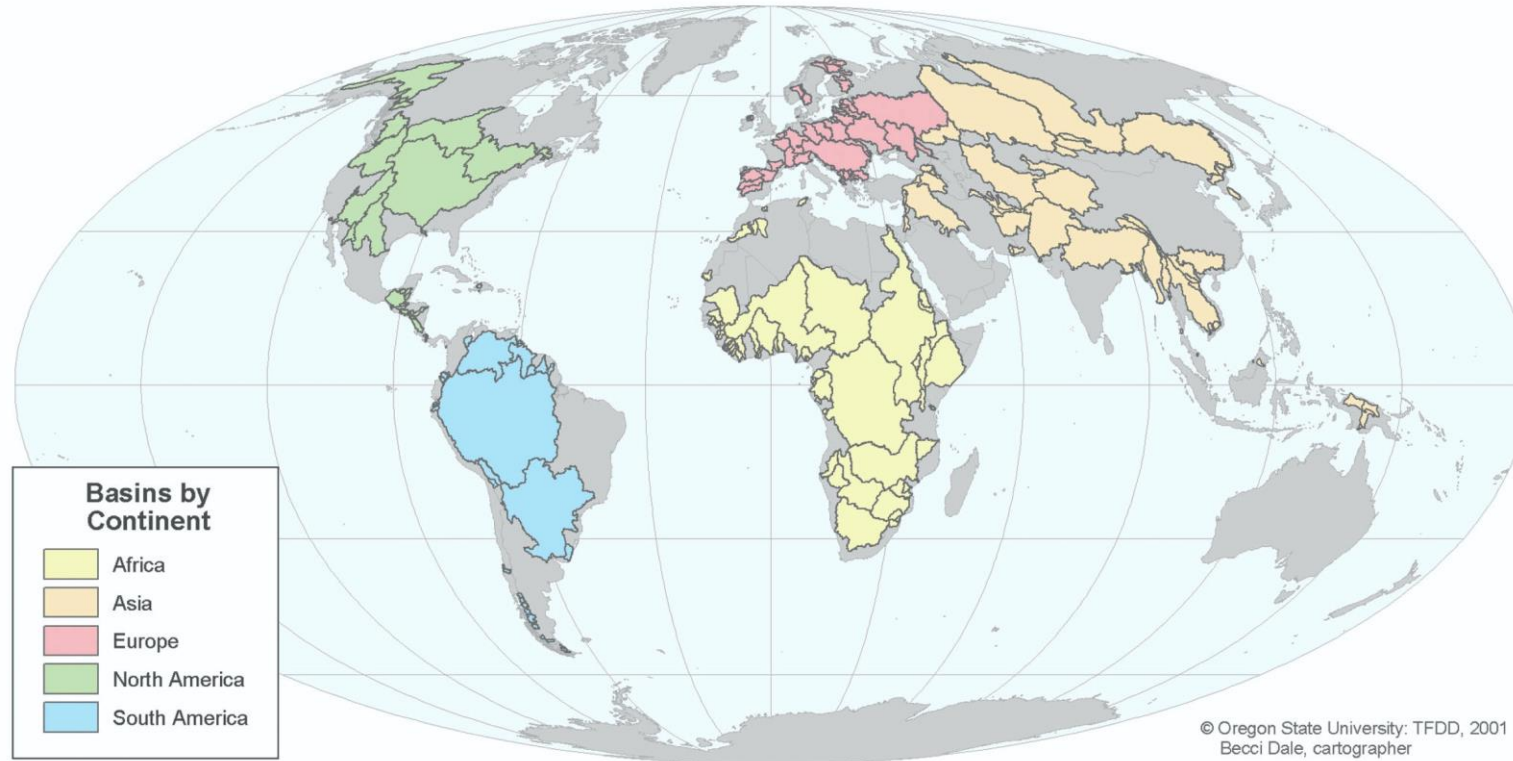
Using Satellite Observations to Address Power Asymmetries in Transboundary River Basins

by **Vu Trung Dung**
under the guidance of **Assoc. Prof. Stefano Galelli**
and **Dr. Thanh Duc Dang**

26 July 2021



Transboundary River Basins



© Oregon State University: TFDD, 2001
Becci Dale, cartographer
Image adapted from *Atlas of International Freshwater Agreements*, 2002, UNEP

~**300** transboundary river basins
shared by ~**150** countries

~**50%** of the world's land surface
(McCracken and Wolf, 2019)

~**60%** of the global river flow
(Wolf et al., 2005)



“ Transboundary river basins are river basins **shared by two or more countries**, which supports the lives and livelihoods of vast numbers of people across the riparian countries. ”

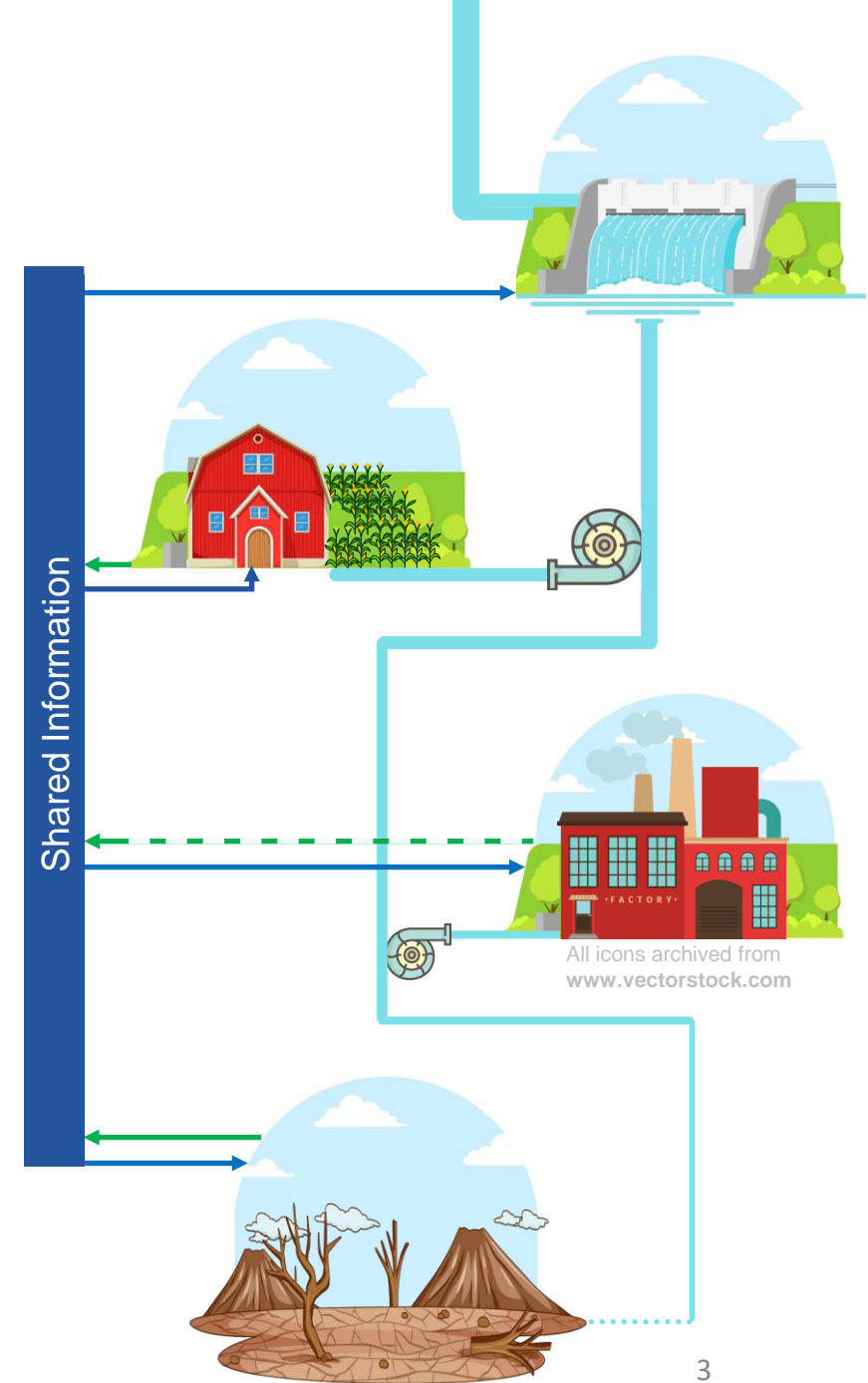
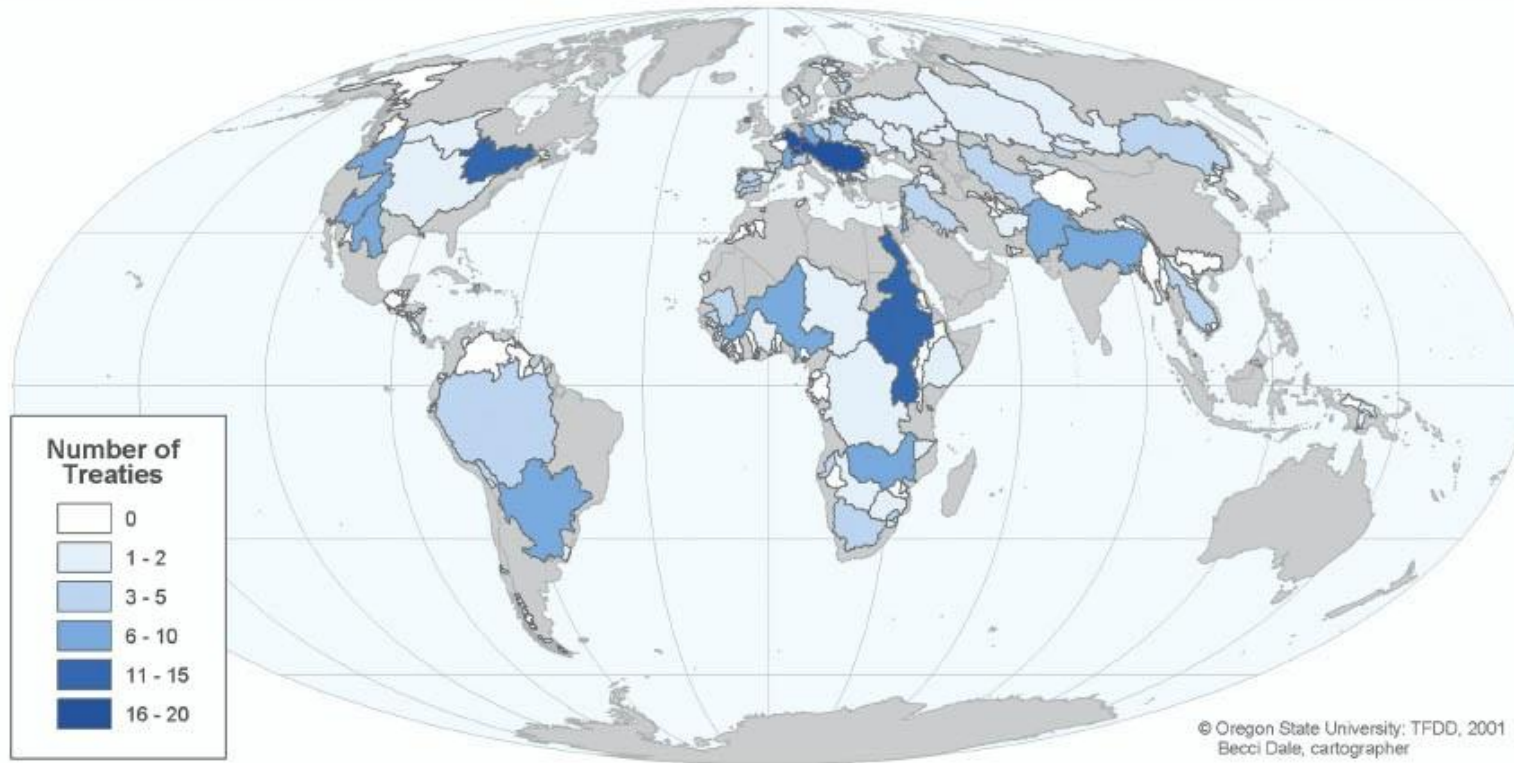


“ The potential for **conflict** over shared water resources is real, so it is important that countries reach **agreement**. ”

“ To mitigate the likelihood of conflict as well as to resolve existing disputes, the international community has devised **principles** for international watercourse management. ”

“ Basin communities have built their own **treaties**. ”

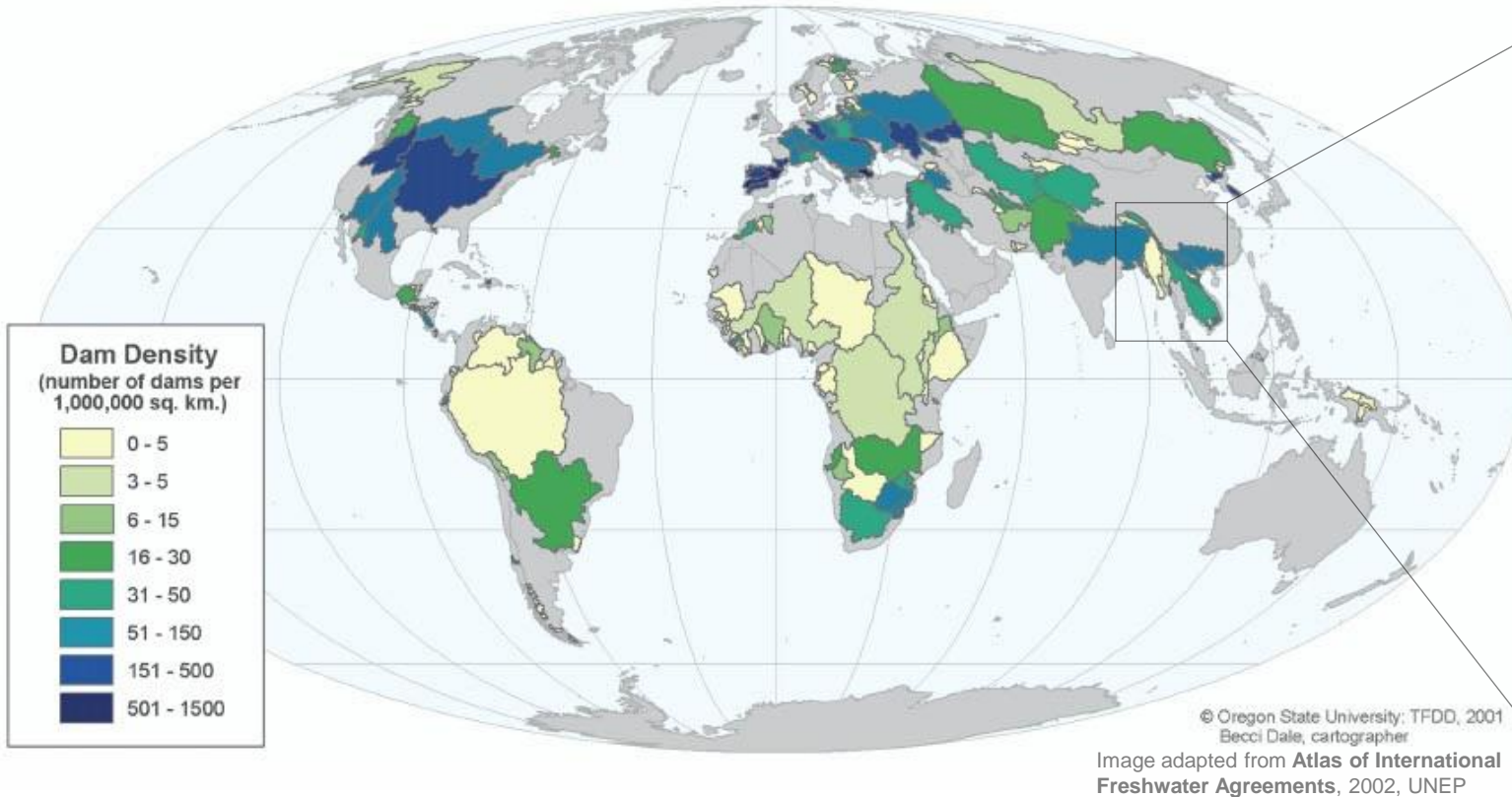
Number of Agreements per Transboundary River Basin



Different views on [how the transboundary water should be used
+ **Natural power asymmetry** between upstr. and downstr. countries

 Environmental and socio-economic **impacts** in **downstream areas**

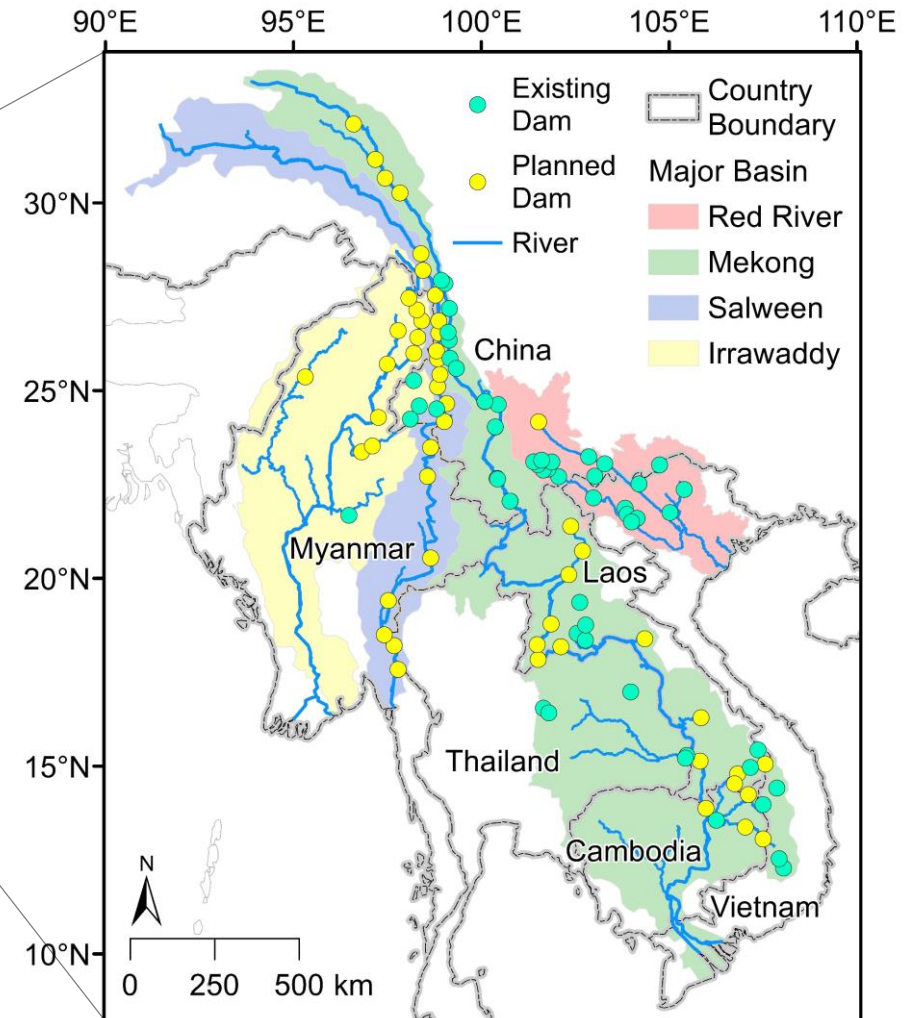
Dam Density per Transboundary River Basin



Many existing and planned dams → downstream countries are increasingly dependent on upstream ones

But there is **no shared platform** providing a **detailed** and **complete** accounting of the amount of water stored and released by large dams

Problem: No shared data ← **Solution: Satellite observations**



Hydropower development in the transboundary river basins of Southeast Asia

Data source: Global Reservoir and Dam Database (GRanD)



United States Geological Survey



National Aeronautics and Space Administration, US



National Centre for Space Studies, France



European Space Agency

Landsat

Operation Period	1972-now
Temporal Resolution(s)	16 days
Spatial Resolution(s)	30, 60 m

MODIS

Operation Period	1999-now
Temporal Resolution(s)	1 day
Spatial Resolution(s)	250 m

Sentinel

Operation Period	2014-now
Temporal Resolution(s)	10, 12, 17 days
Spatial Resolution(s)	5, 10, 300 m

Jason

Operation Period	2002-now
Temporal Resolution(s)	10 days

Envisat

Operation Period	2002-2010
Temporal Resolution(s)	35 days

Imagery



Water Surface Area (WSA)

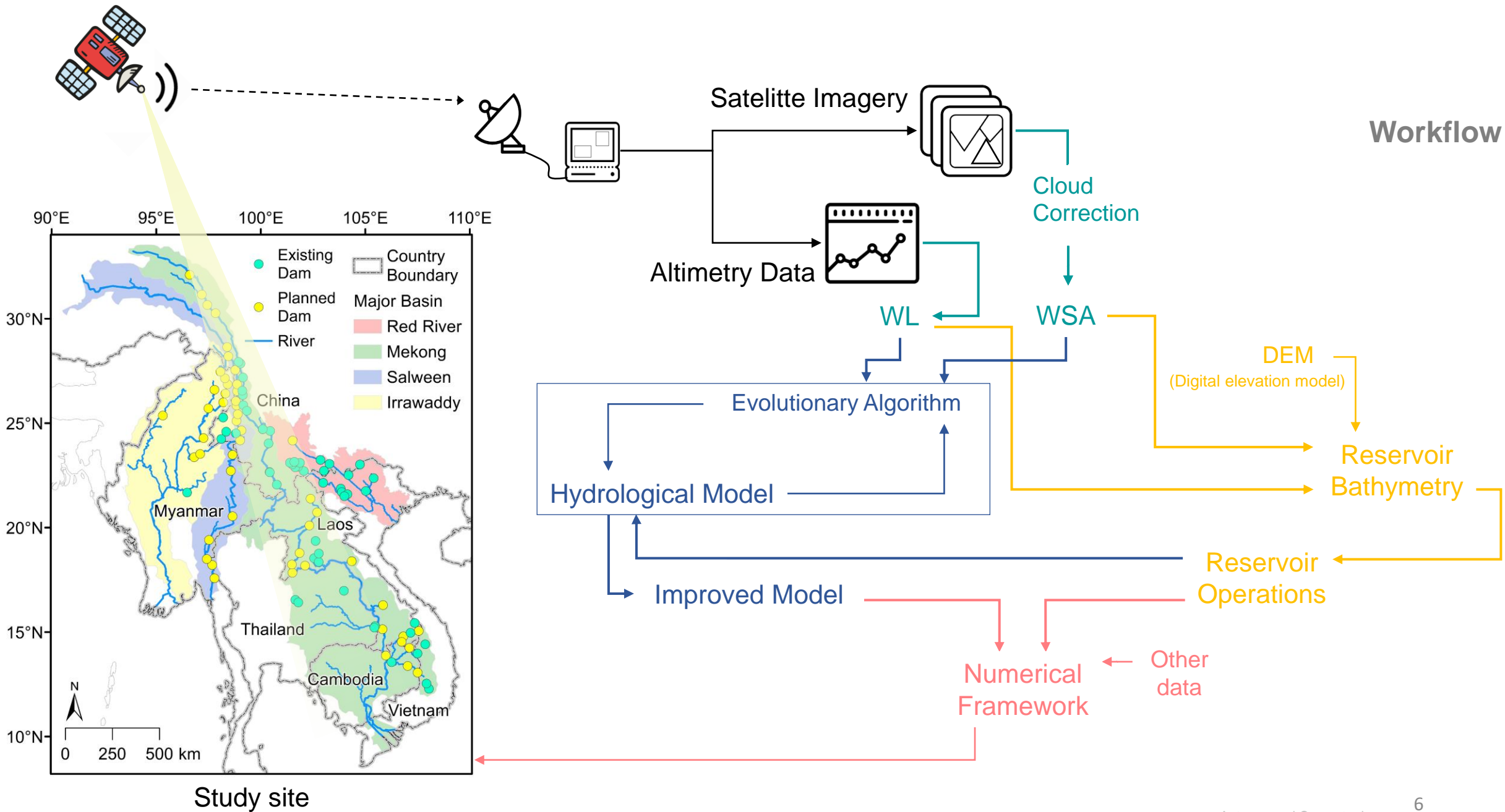


Altimetry



Water Level (WL)

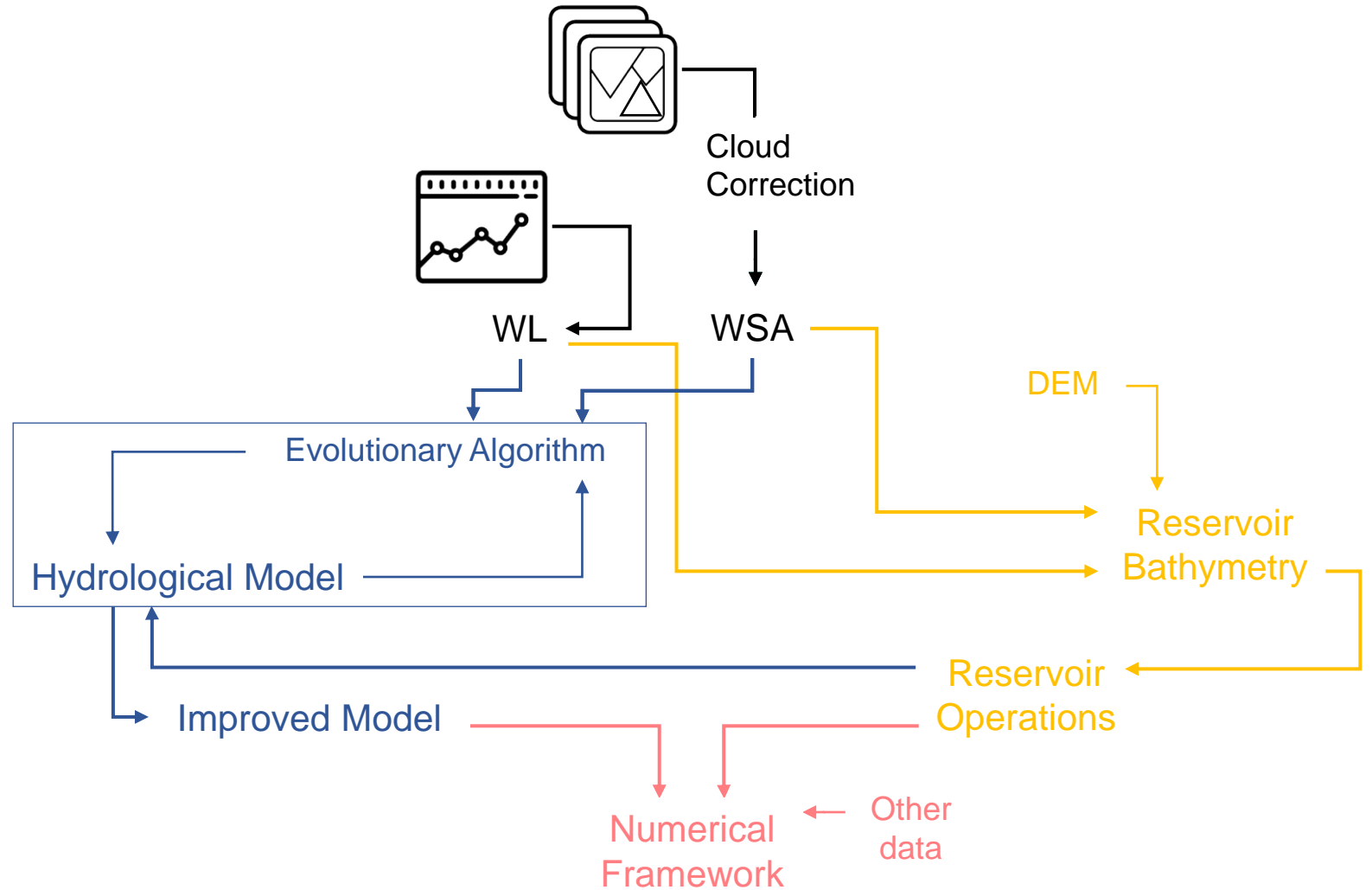




Inferring reservoir **storage variations**, filling strategies, and operating rules from **satellite observations**

Improving reliability of large-scale **hydrological models** with **satellite observations**

Using **satellite-derived data** to support **downstream countries** in water resources management





SINGAPORE UNIVERSITY OF
TECHNOLOGY AND DESIGN

(1)



UNIVERSITY of
SOUTH FLORIDA

(2)



UNIVERSITY of
WASHINGTON

(3)

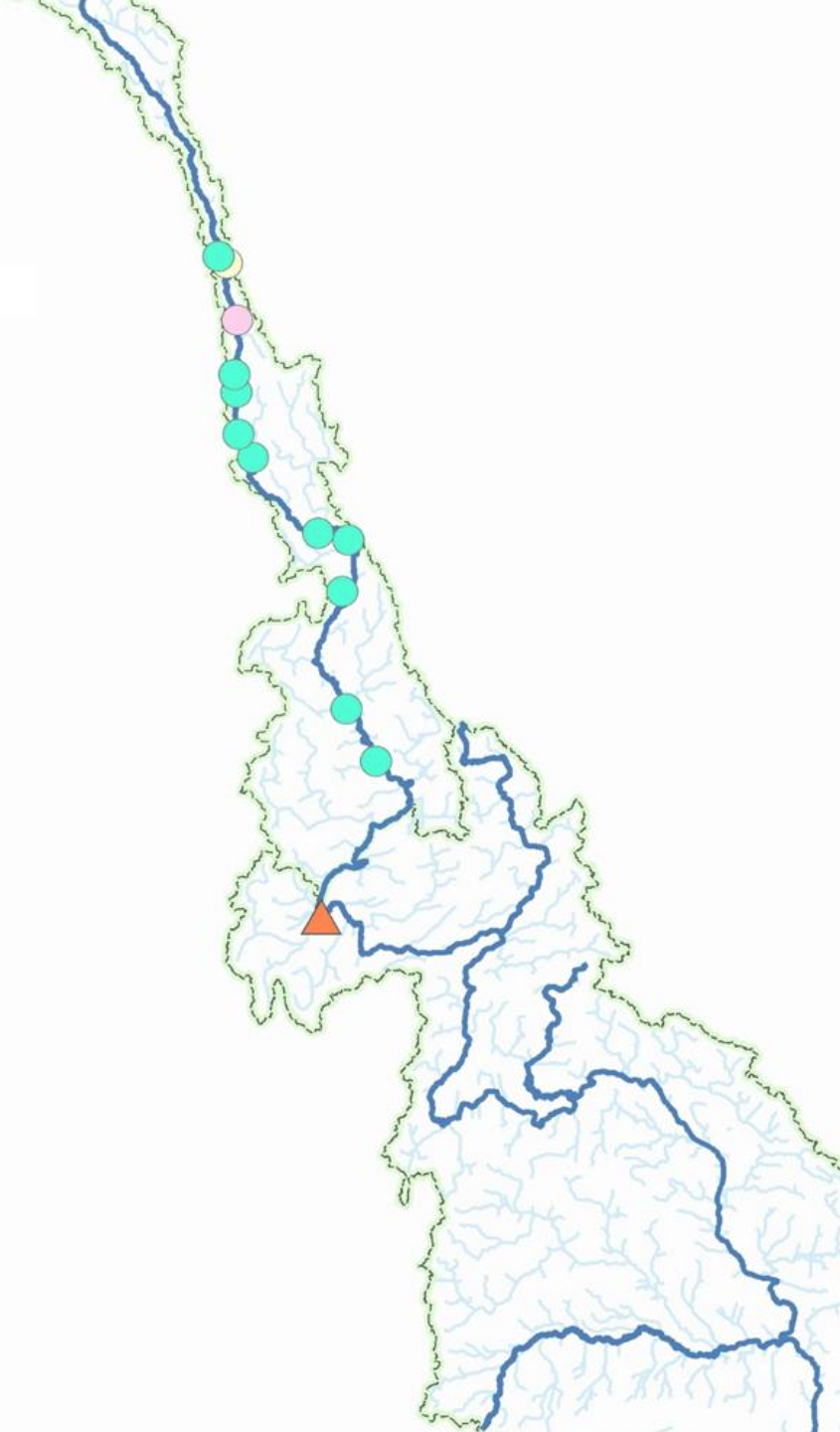
Satellite Observations Reveal Thirteen Years of Reservoir Filling Strategies, Operating Rules, and Hydrological Alterations in the Upper Mekong River Basin

Dung Trung Vu¹, Thanh Duc Dang^{1,2}, Stefano Galelli¹, and Faisal Hossain³

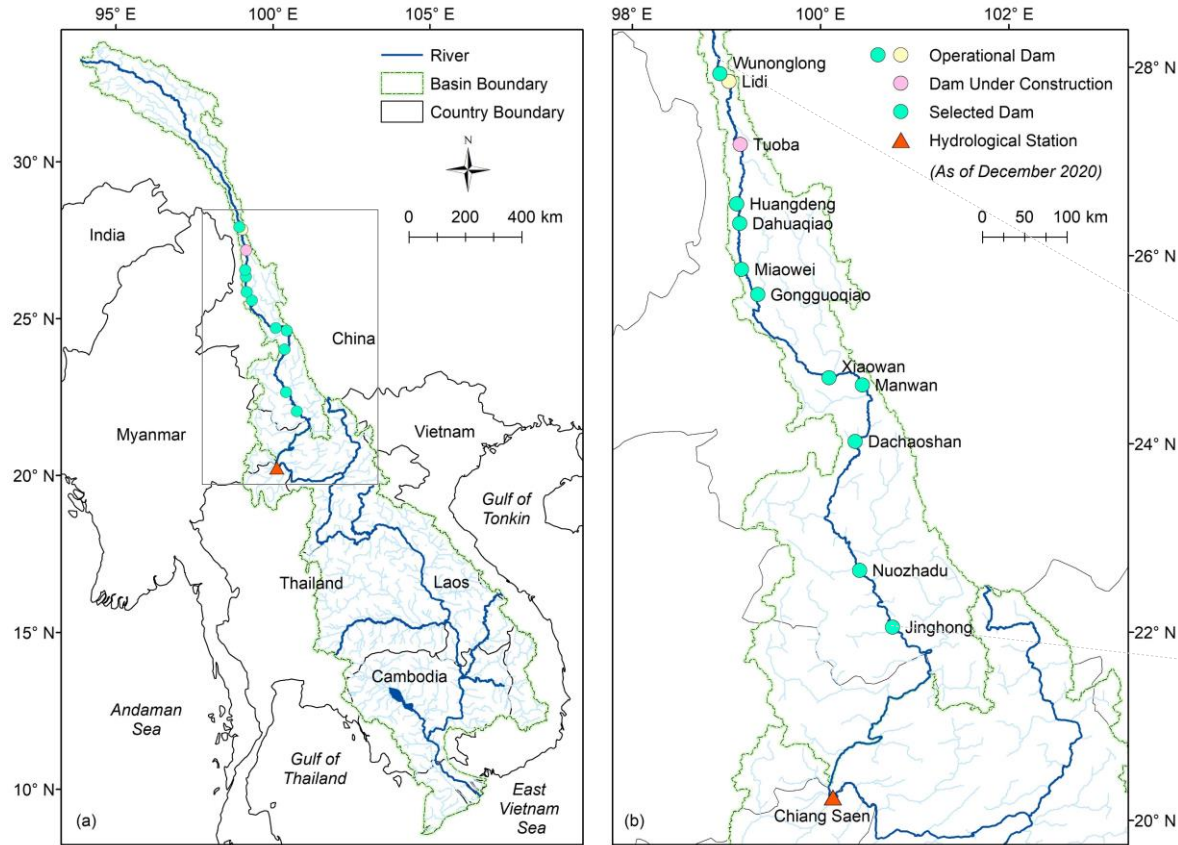
Submitted to Hydrology and
Earth System
Sciences



on 6 July 2021



Problem Statement

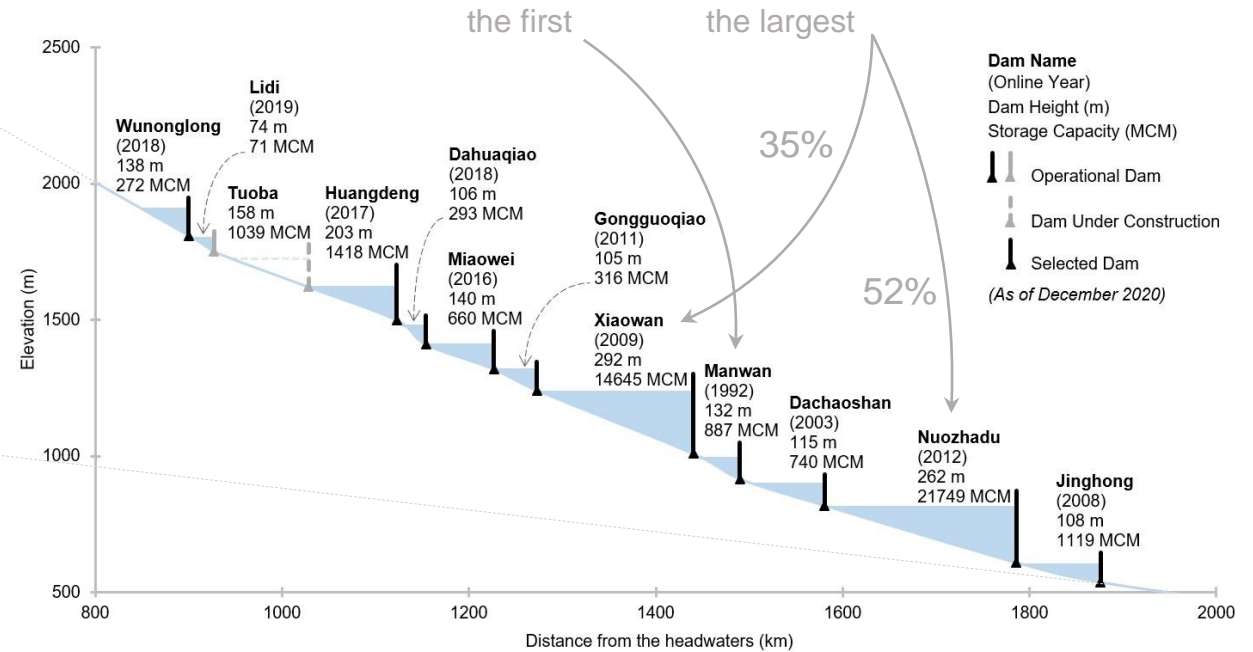


Mekong River Basin (a) and its upper portion (the Lancang River Basin) and location of the hydropower dams on the mainstream (b)

10 large dams
 volume ≥ 100 MCM
 (each)

total volume
 > 42000 MCM

control $\sim 40\%$
 of the annual flow
 at **Chiang Saen**



Cascade reservoir system on the Lancang River

Data source: Do et al. (2020)

Water withheld in the dams \rightarrow source of **controversy**
 between China and downstream countries

Assessing real impacts of the dams = a **challenging** task
lack of data on reservoirs storage and operations

Mekong Dam Monitor

Launched in 12/2020

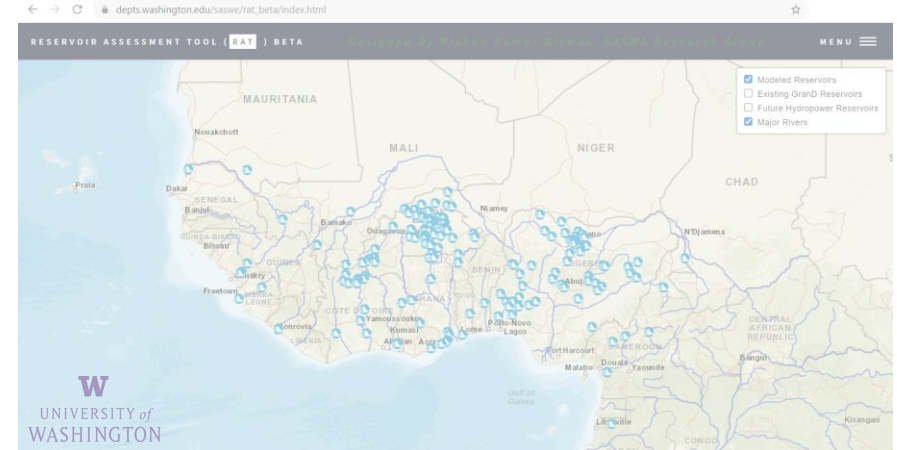


Sentinel (2014)
Mekong River
11 reservoirs in Lancang
Does not include the filling period of Nuozhadu and Xiaowan

Landsat (1984)
South America, Africa, and SEA
6 reservoirs in Lancang
Discontinuous data due to cloud cover on images

Reservoir Assessment Tool

Beta version



Open Access Article

Assessment of the Impact of Reservoirs in the Upper Mekong River Using Satellite Radar Altimetry and Remote Sensing Imageries

Kuan-Ting Liu, Kuo-Hsin Tseng, C. K. Shum, Chian-Yi Liu, Chung-Yen Kuo, Ganming Liu, Yuanyuan Jia, and Kun Shang

2016, Volume 8, Issue 5, Pages 367, doi: [10.3390/rs8050367](https://doi.org/10.3390/rs8050367)

Landsat (1972)
Jason (2002) and Envisat (2002)
2 dams in Lancang
Cloud cover and Altimetry availability

MODIS (1999)
ICESat (2003)
South Asia

Only applicable for large reservoirs
low resolution images (250m)
low density of Altimetry data (4/year)
Image enhancement algorithm

Water Resources Research



Research Article | [Free Access](#)

Monitoring reservoir storage in South Asia from multisatellite remote sensing

Shuai Zhang, Huilin Gao, and Bibi S. Naz

2014, Volume 50, Issue 11, Pages 8927-8943,
doi: [10.1002/2014wr015829](https://doi.org/10.1002/2014wr015829)

Need **continuous** time-series data of (at least) **monthly** storage of reservoirs (including **small size** and **unusual shape** ones) covering period **2009-current** (at least)

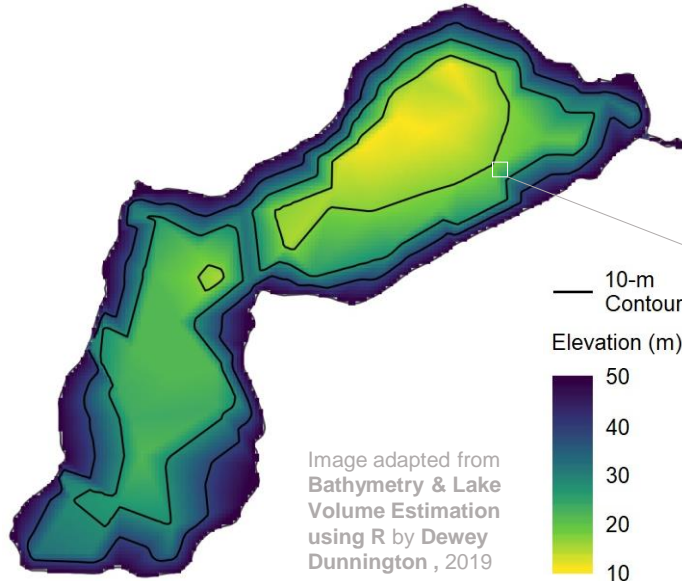


Landsat require an image enhancement process to remove cloud cover effect



Make use of all available **Altimetry** data for validation purpose

Methodology



SRTM DEM

(Shuttle Radar Topography Mission)
Jet Propulsion Laboratory, NASA
11 - 22 February 2000

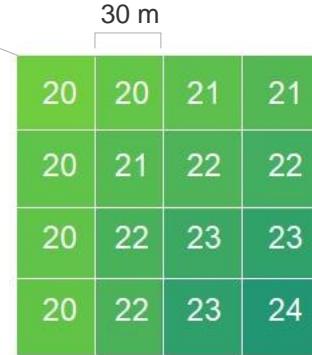
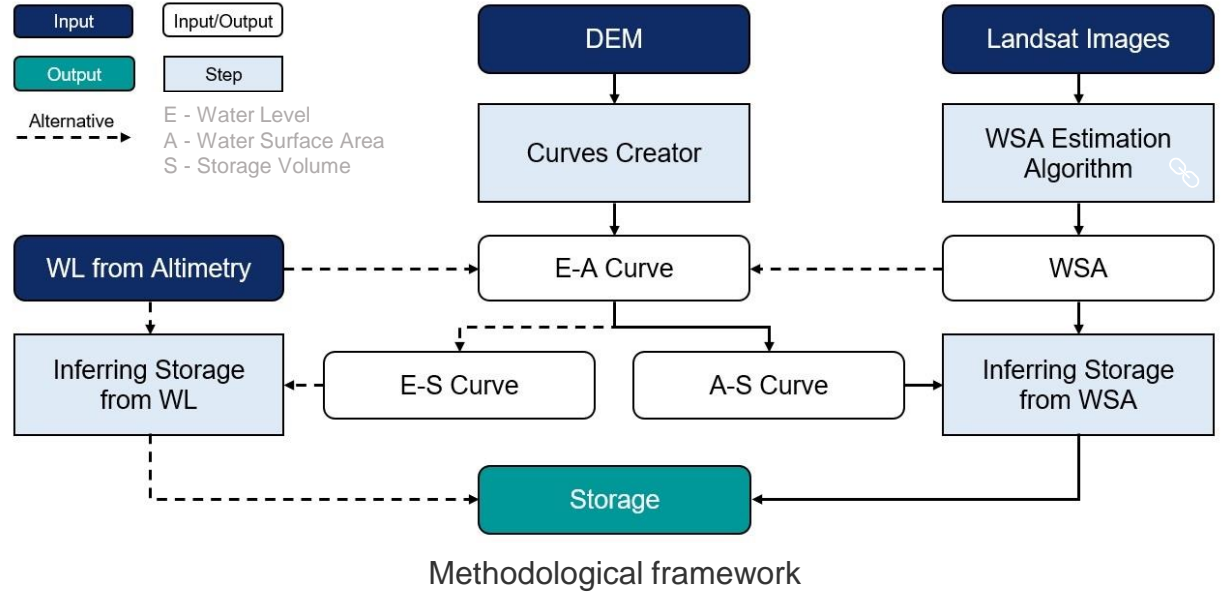
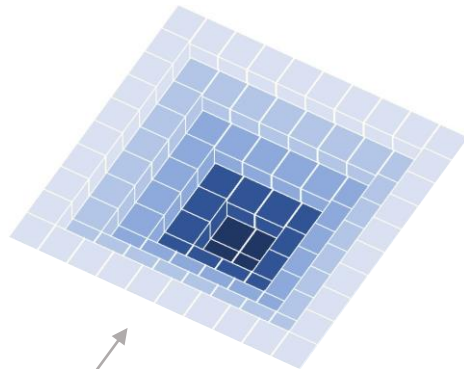
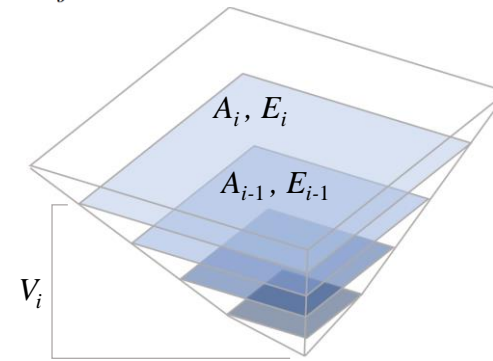
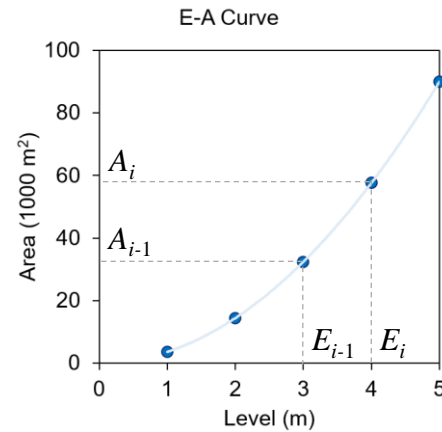


Image adapted from
Bathymetry & Lake
Volume Estimation
using R by Dewey
Dunnington, 2019

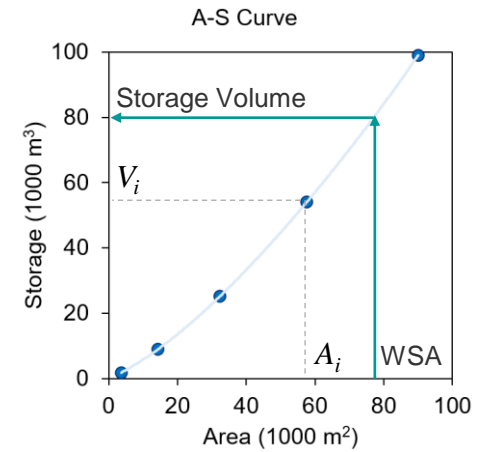
5	5	5	5	5	5	5	5	5	5	5
5	4	4	4	4	4	4	4	4	4	5
5	4	3	3	3	3	3	3	3	4	5
5	4	3	2	2	2	2	2	3	4	5
5	4	3	2	1	1	2	3	4	5	
5	4	3	2	1	1	2	3	4	5	
5	4	3	2	2	2	2	3	4	5	
5	4	3	3	3	3	3	3	4	5	
5	4	4	4	4	4	4	4	4	5	
5	4	4	4	4	4	4	4	4	5	
5	5	5	5	5	5	5	5	5	5	



$$V_i = \sum_{j=l}^i (A_j + A_{j-1})(E_j - E_{j-1})/2$$







$E_i - E_{j-1} = 1$ (for SRTM DEM)
e.g.: $i = 4, l = 1, A_{l-1} = 0$







Data Availability & Code

Input data

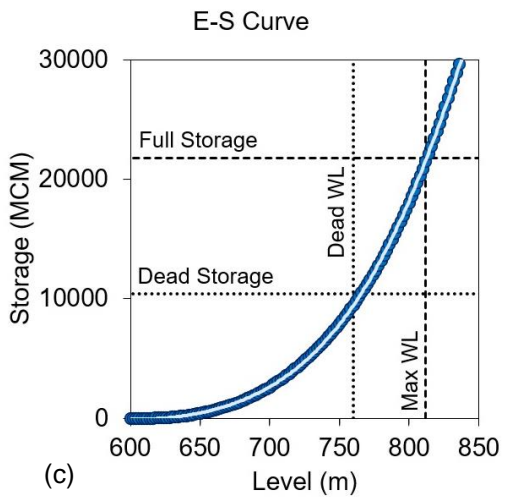
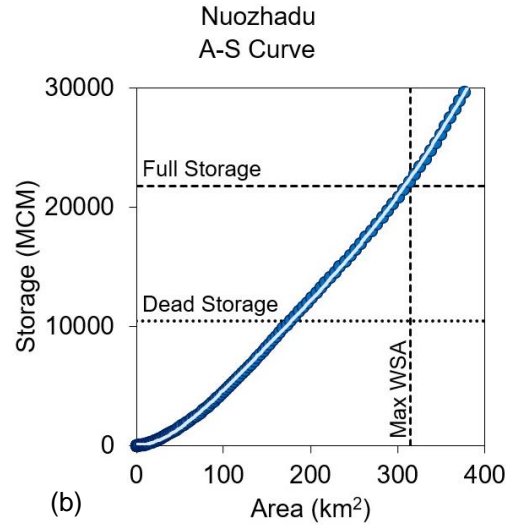
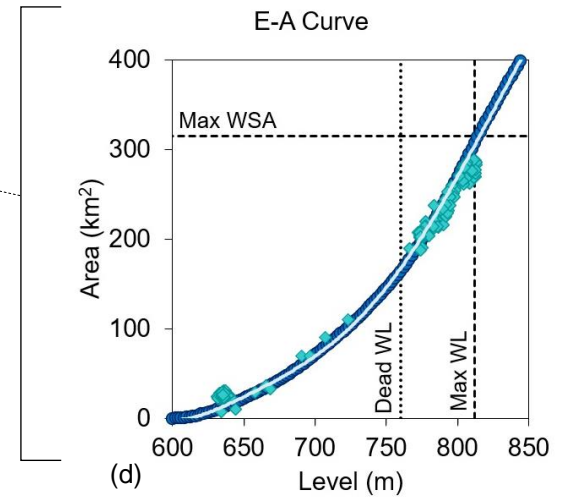
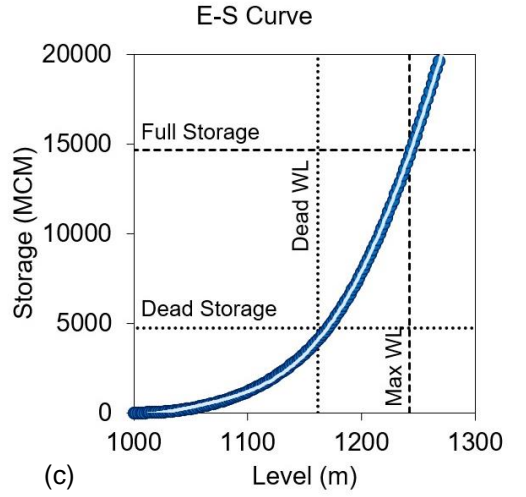
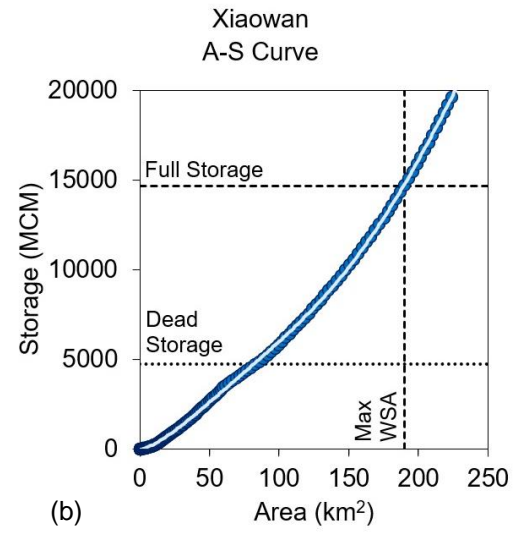
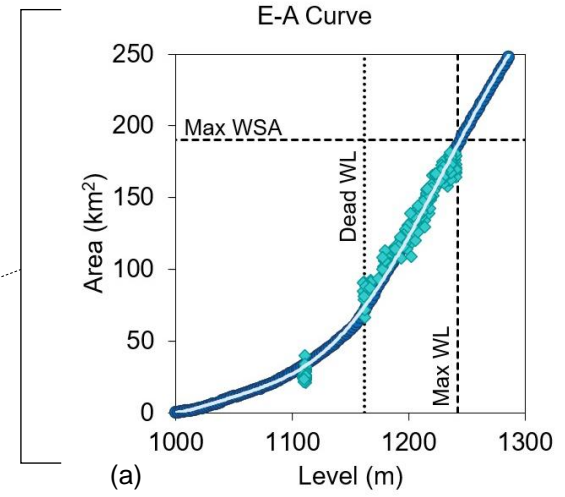
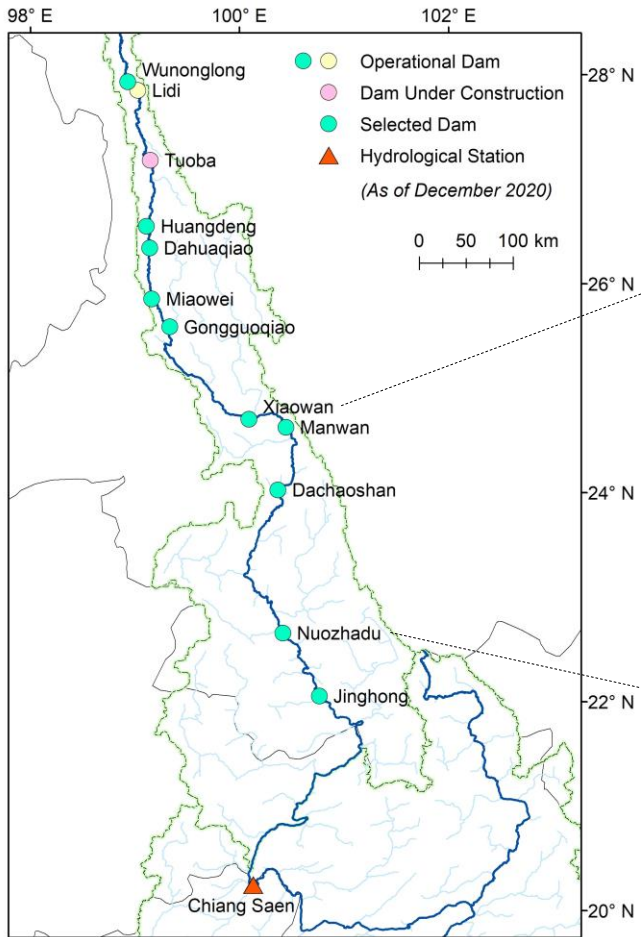
Data		Source
SRTM DEM Landsat images		United States Geological Survey (USGS) earthexplorer.usgs.gov/
Jason Altimetry data		Global Reservoirs and Lakes Monitor (G-REALM) United States Department of Agriculture (USDA) ipad.fas.usda.gov/cropexplorer/global_reservoir/
Daily discharge data at Chiang Saen		Mekong River Commission (MRC) portal.mrcmekong.org/
CHIRPS 2.0 precipitation data		University of California, Santa Barbara data.chc.ucsb.edu/products/CHIRPS-2.0/

Output data and Code are available at  [GitHub.com/dtvu2205/210520](https://github.com/dtvu2205/210520)

Code file	Function	Used Library
Py_Curve	Create the Water Level - Water Surface Area - Storage Volume curves of reservoirs from DEM	 OSGeo Open Source Geospatial Foundation
 Py_Mask	Create the expanded mask and zone mask of reservoirs	 
Py_WSA	Estimate reservoir water surface area from Landsat images	

Results

E-A, A-S, and E-S Curves

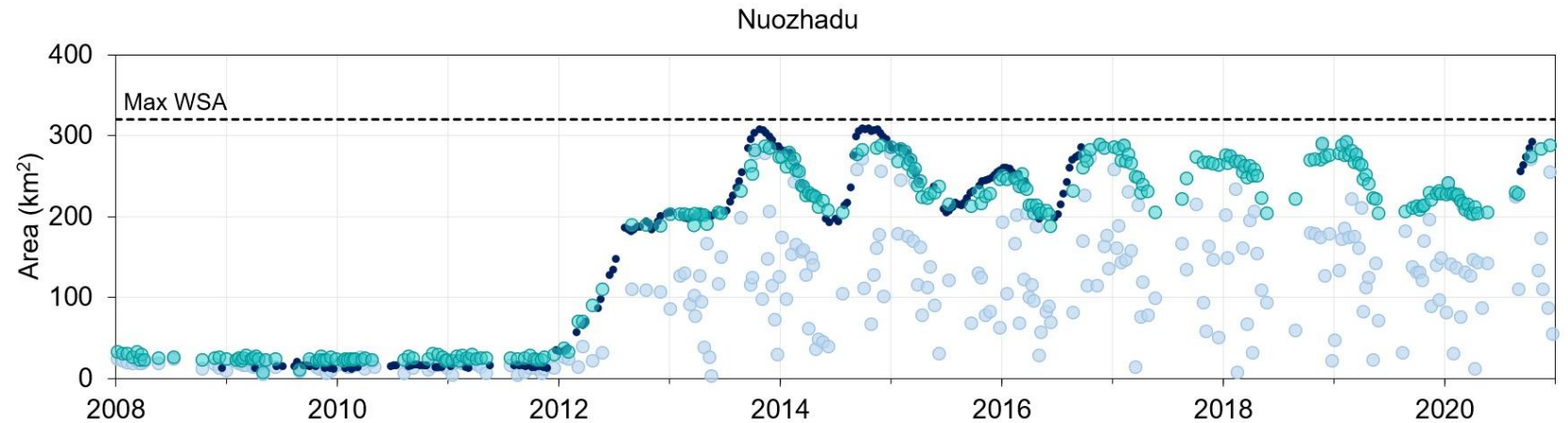
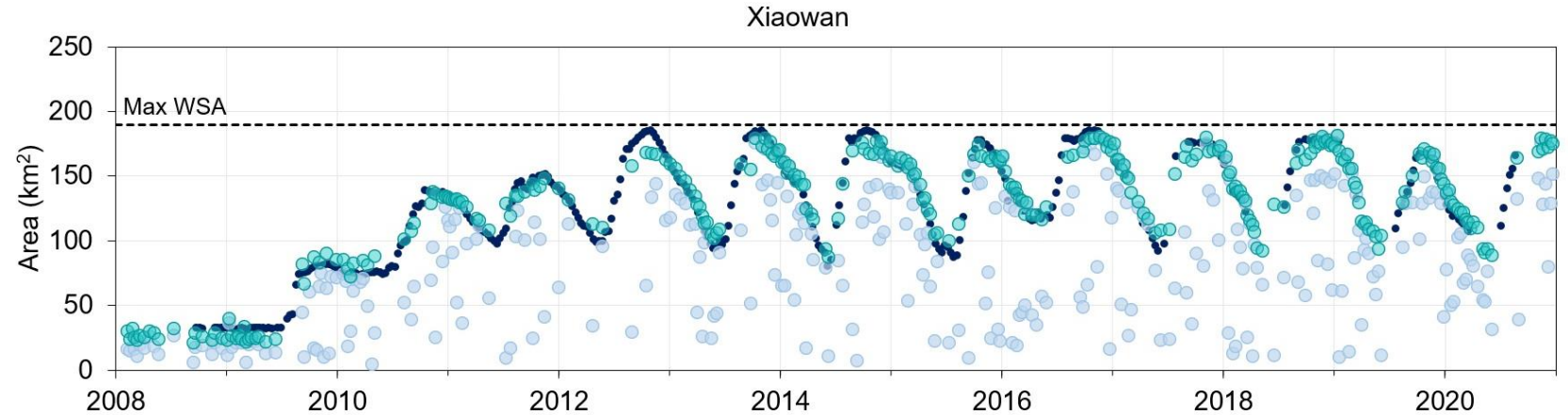
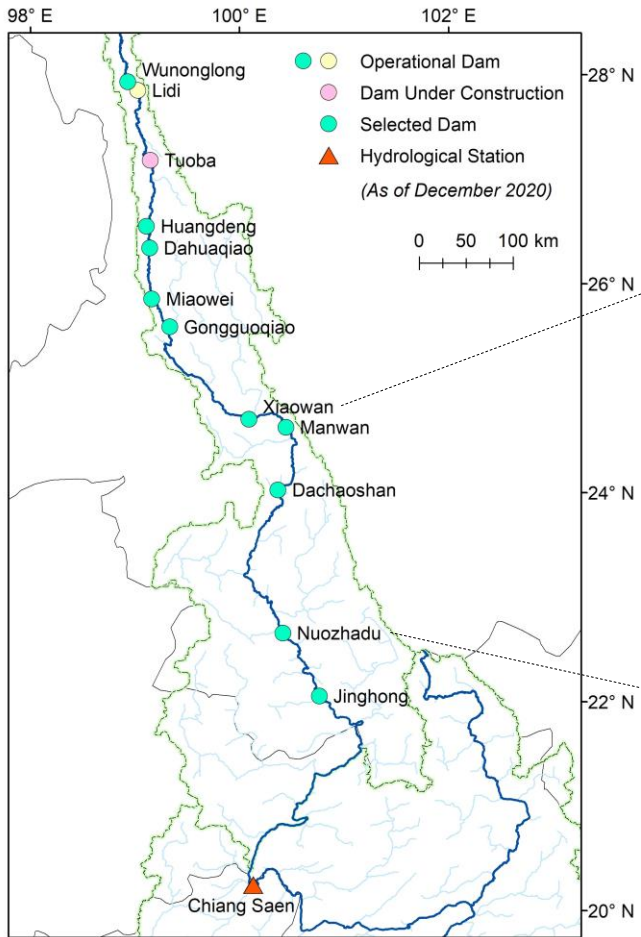


● DEM ◆ Pairing — DEM-fitted

Reservoir's specifications archived from Do et al. (2020)

Results

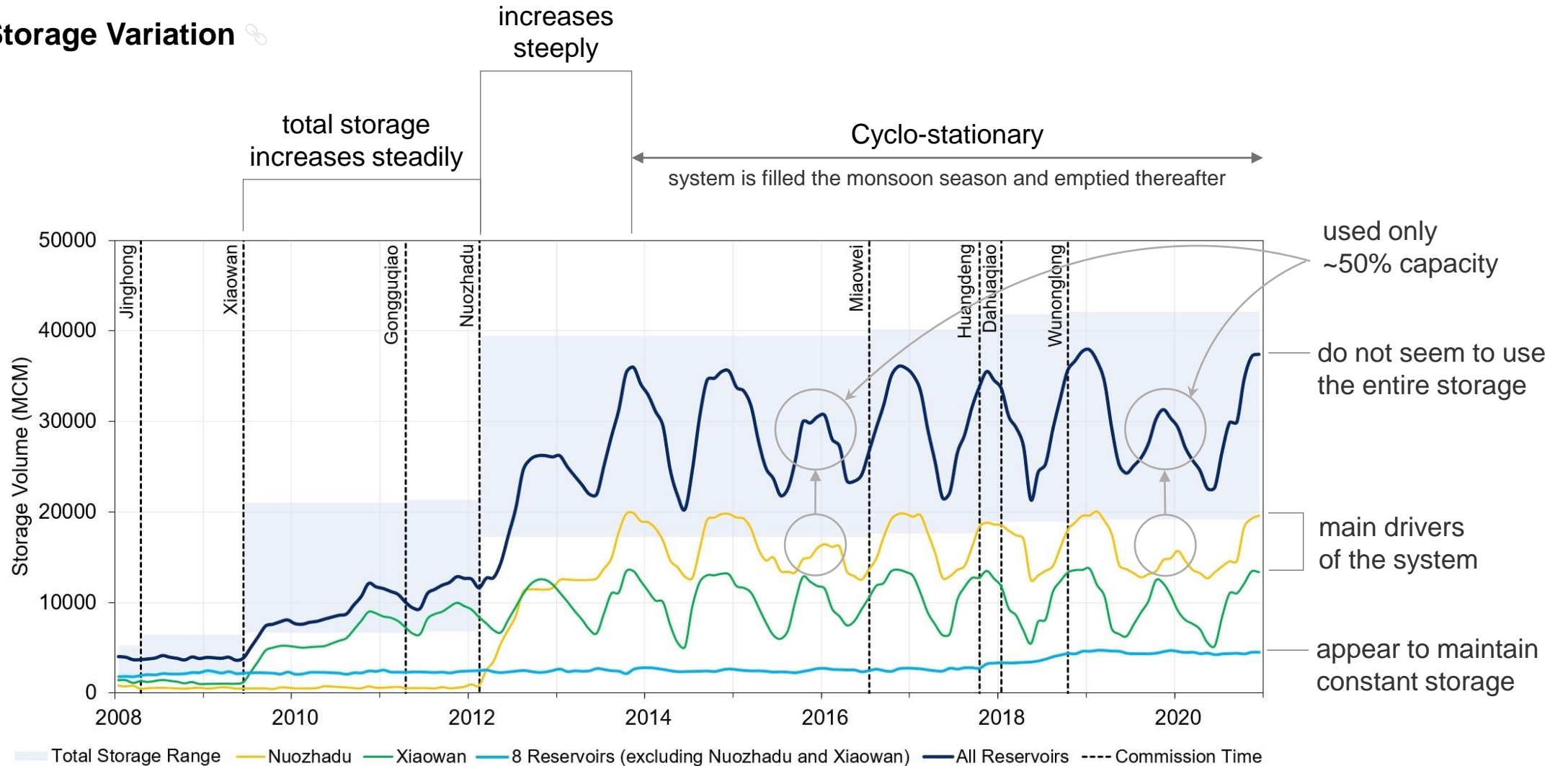
Reservoir Water Surface Area



• Altimetry-converted • Landsat-derived (before improvement) • Landsat-derived (after improvement)

Results

Reservoir Storage Variation



Storage variation range of the whole reservoir system (constrained by dead and full storage volume) and the storage variation of Nuozhadu, Xiaowan, 8 other reservoirs, and all 10 reservoirs

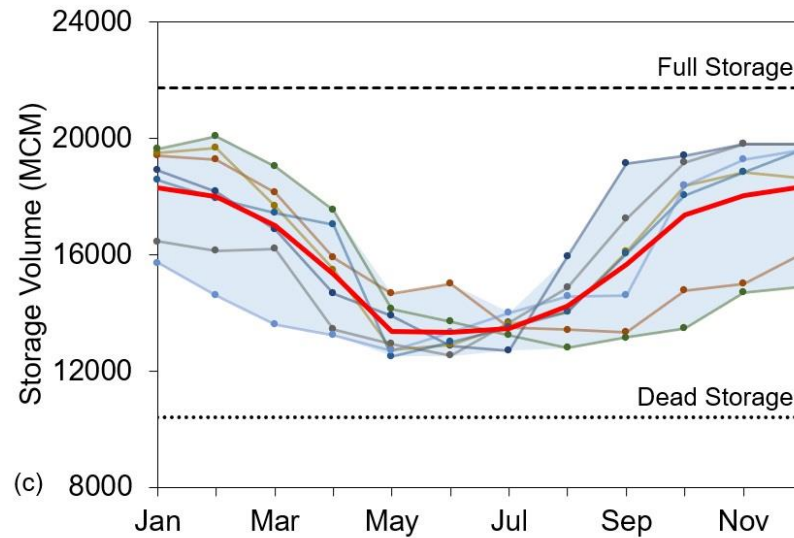
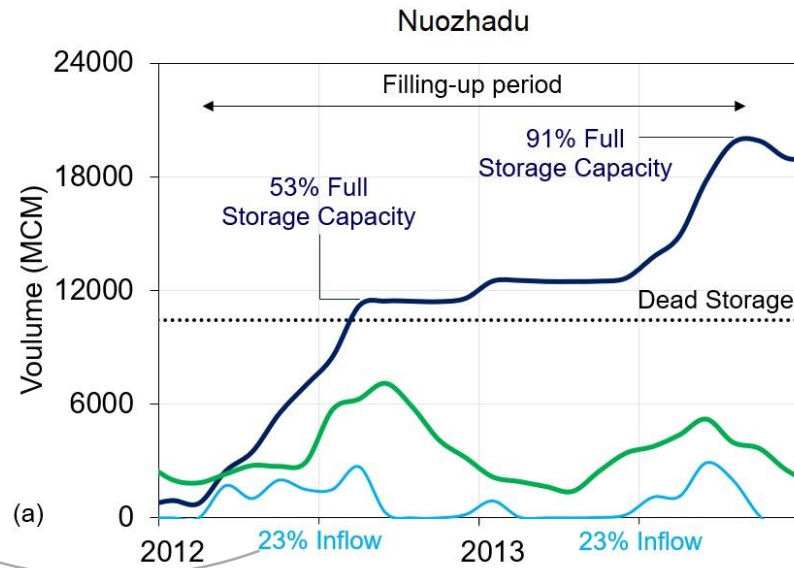
Results

∞ Filling Strategies

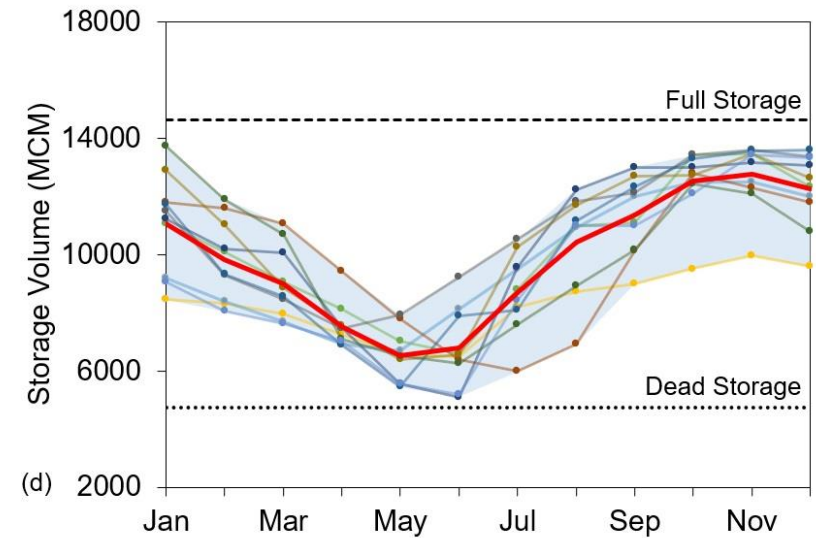
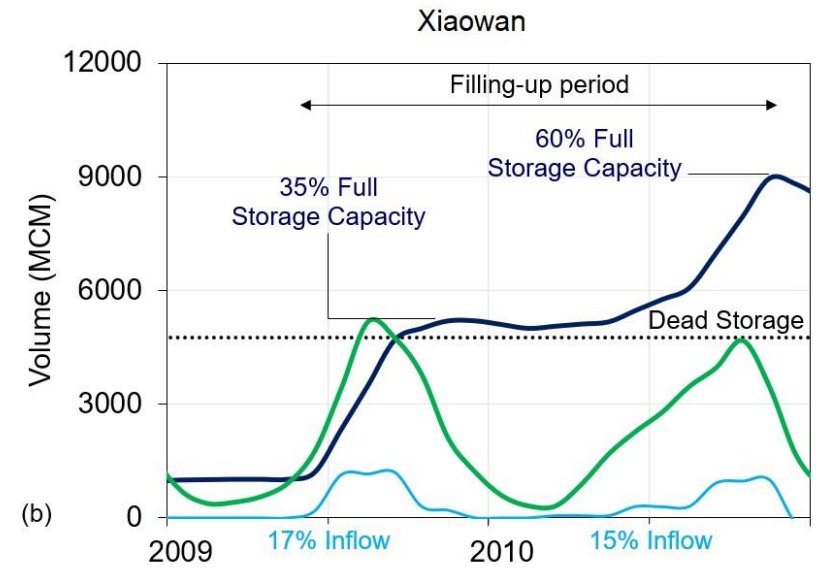
The fraction of inflow that is retained by the reservoir on a periodic basis

~9900 MCM ~12% of the average annual discharge at Chiang Saen

∞ Operation Curves



— Inflow (by VIC-Res) — Storage (by Landsat)
 — 2011 — 2012 — 2013 — 2014 — 2015



— Storage Change — Average Storage
 — 2016 — 2017 — 2018 — 2019 — 2020

Results

Impacts of Reservoir Operations on the Discharge Downstream

Hydrological Alteration Index

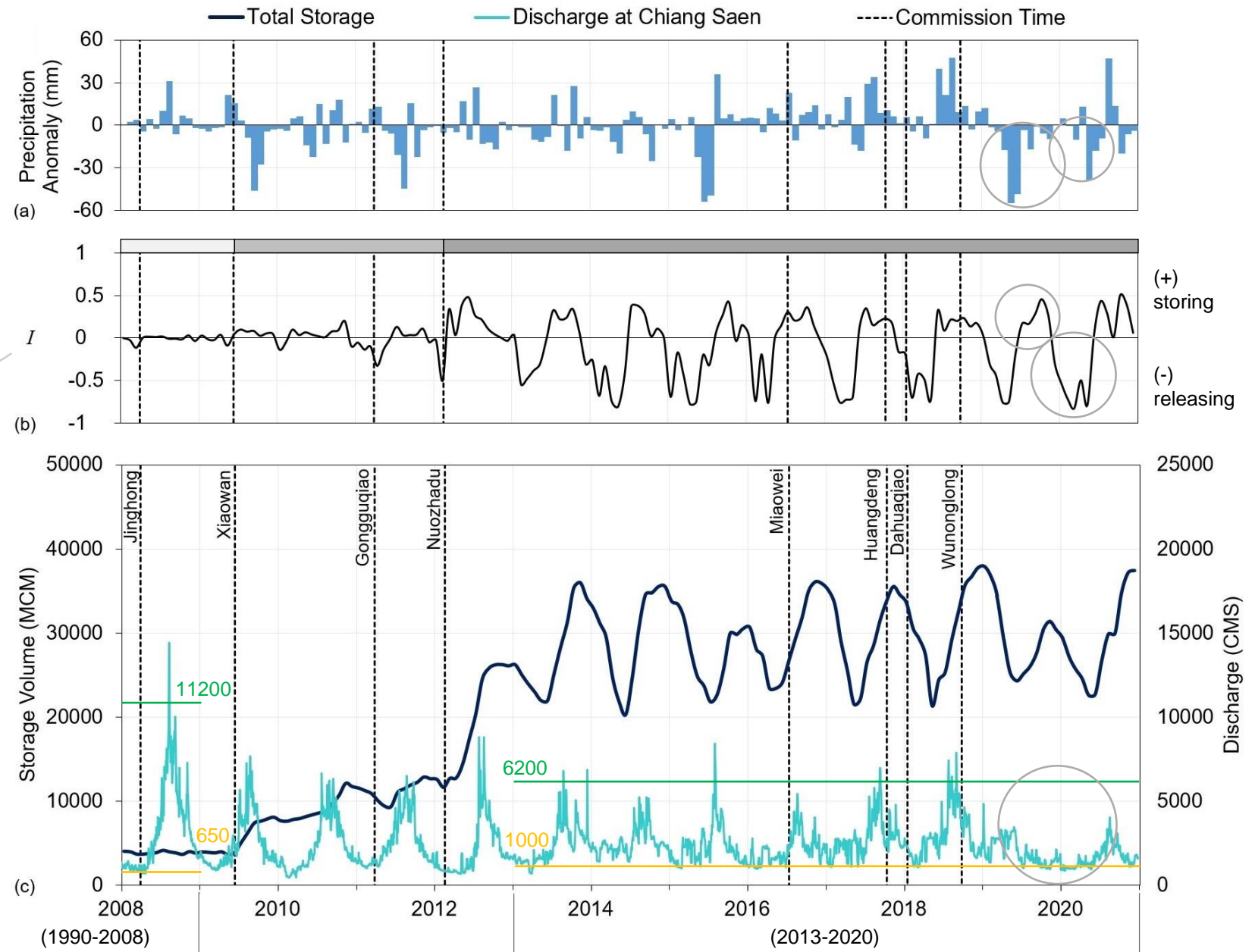
$$I_t = \frac{\Delta S_t}{\Delta S_t + Q_t} \quad , \quad \Delta S_t = S_t - S_{t-1}$$

S_t : storage on day t

ΔS_t : storage change between day t and $t-1$

Q_t : observed discharge at downstream on day t

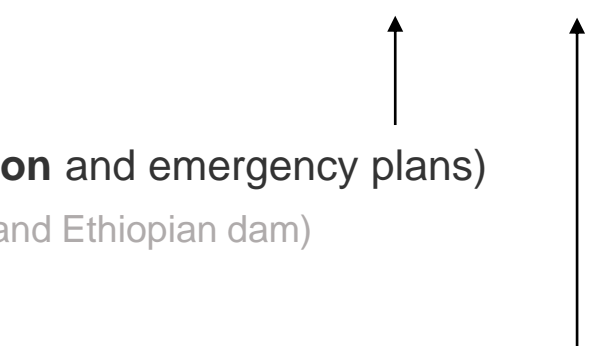
$\Delta S_t + Q_t \sim$ estimated natural flow discharge at ds



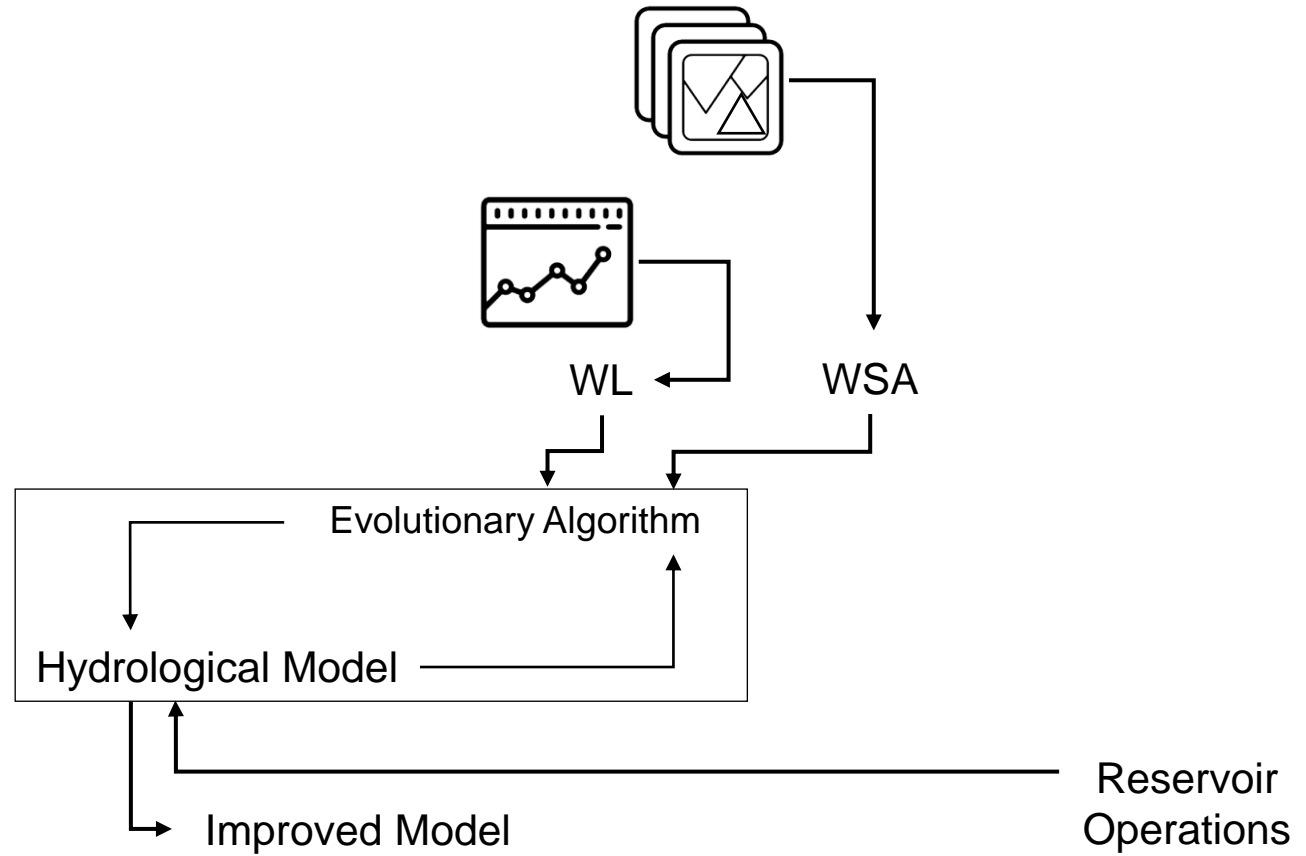
Discussions and Conclusions



- Study produced a **monthly storage TS** for each of **10 large reservoirs** in the Lancang River for **13 past years**, described the **evolution** of the dam cascade system, and highlighted the **pivotal role** of Xiaowan and Nuozhadu
- **Operating rules** could be incorporated to hydrological model of downstream countries → Address the **asymmetric** relation between countries
+ and benefit for Mekong's wetland and delta downstream
nearly **real-time** storage **monitoring**
- **Filling strategies** is important to prepare for future infrastructural changes (**adaptation** and emergency plans) can be used when **negotiating** the filling of new dams (e.g.: the Grand Ethiopian dam)
- **Reservoir operations** could improve the existing **large-scale hydrological models** which exclude reservoir operations or use generic operation schemes
+ remote-sensed WL and WSA



Improving reliability of large-scale **hydrological models** with **satellite observations**



A **generic inflow-and-demand-based** release scheme is deployed, rather than its record of operation (Turner et al, 2020)

Availability and accessibility of reservoir management data are **major problems**

However, substantial **errors** in simulated releases are **inevitable**. Errors could compound over time through storage memory. Errors could propagate to the reservoirs downstream.

Lack of measured discharge data for model calibration is still a remarkable **problem**

Large-scale Models

Wide-spread due to the need to manage sustainably large river basins and global environmental changes

Large-scale Models

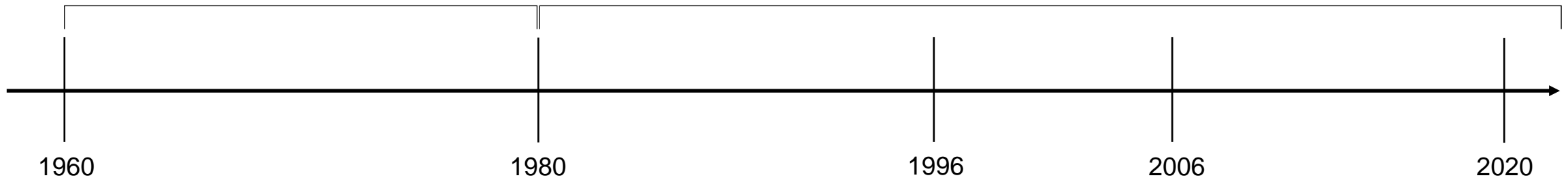
with human-water interaction especially **reservoir operations** since their absence affects model parameterization (Döll et al., 2008)

Conceptual Models

Simulate behaviors of natural systems through statistical relationship between rainfall and discharge

Distributed Models

Recognized the effects of spatial heterogeneity with spatially varying data (Tang et al., 2006)



Hydrological Model Evolution

On the representation of water reservoir storage and operations in large-scale hydrological models: Implications on model parameterization and climate change impact assessments

Thanh Duc Dang, A. F. M. Kamal Chowdhury, and Stefano Galelli

2020, Volume 24, Issue 1, Pages 397-416, doi: [10.5194/hess-24-397-2020](https://doi.org/10.5194/hess-24-397-2020)

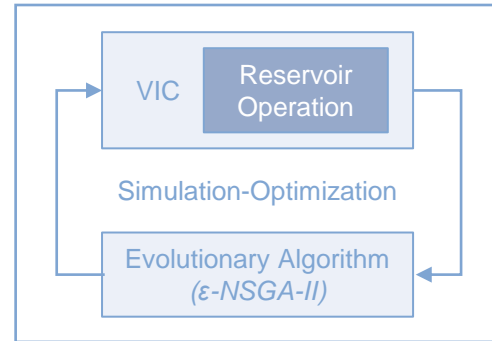


A software package for the representation and optimization of water reservoir operations in the VIC hydrologic model

Thanh D. Dang, Dung T. Vu, AFM K. Chowdhury, and Stefano Galelli

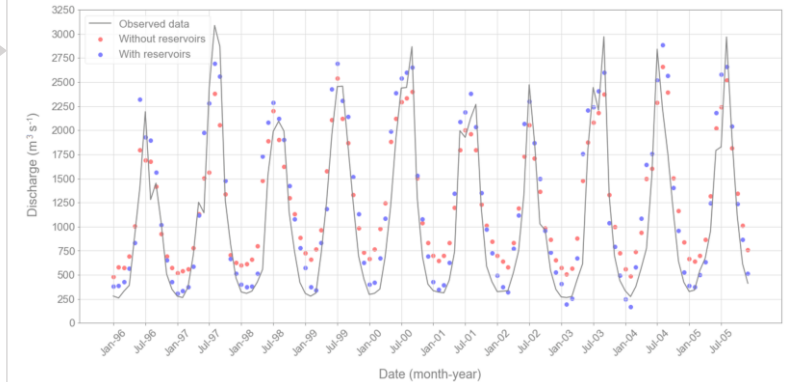
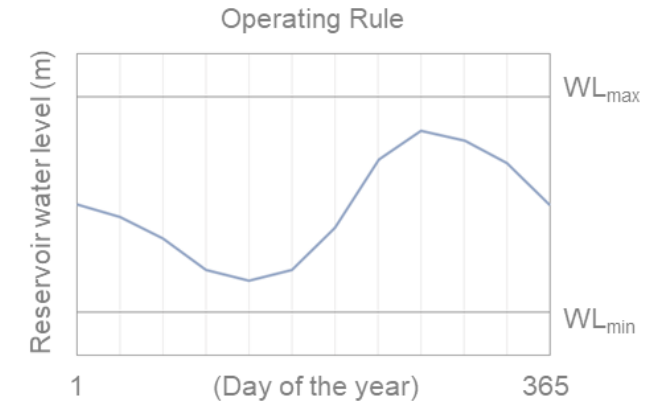
2020, Volume. 126, Pages 104673, doi: [10.1016/j.envsoft.2020.104673](https://doi.org/10.1016/j.envsoft.2020.104673)

VIC-Res



VIC-ResOpt

VIC - Variable Infiltration Capacity
 Macroscale Hydrological Model
 originally developed by Xu Liang
 at the University of Washington



Comparison between observed and simulated monthly discharges at Jiuzhou station (with any without the presence of reservoirs)

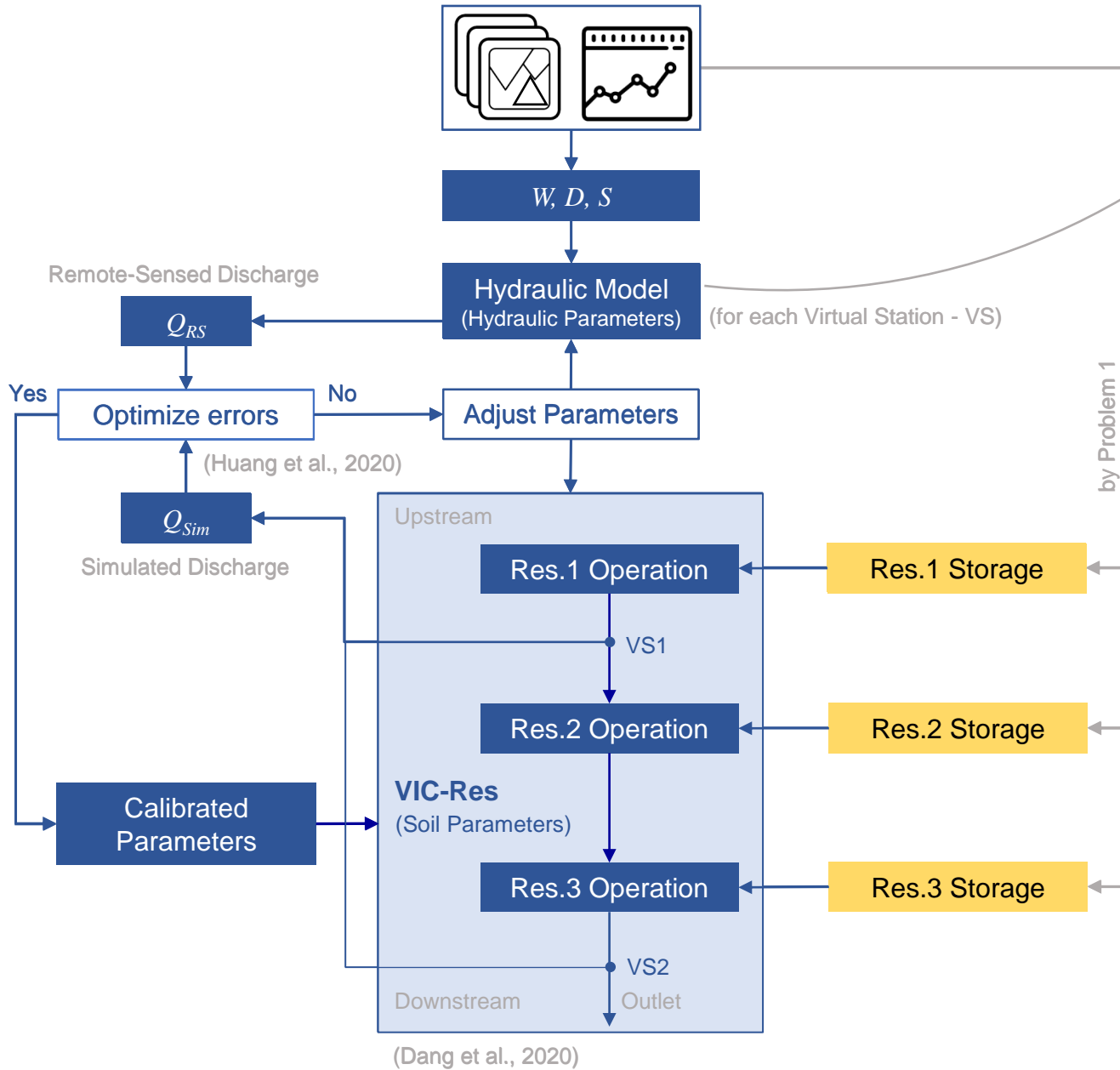
Can we **further improve** the reliability of large-scale hydrological models with the **actual** reservoir operations ?



How to solve the problem of lack of measured discharge data for model calibration ?



Satellite observations



Hydraulic Models

XSECT Hydraulic Model

(Liu et al., 2015)

(XSECT = cross-section)

Manning's equation

$$Q = A_{cross} R^{2/3} S^{1/2} / n, R = A_{cross} / P_{cross} \quad (1)$$

Q - Discharge

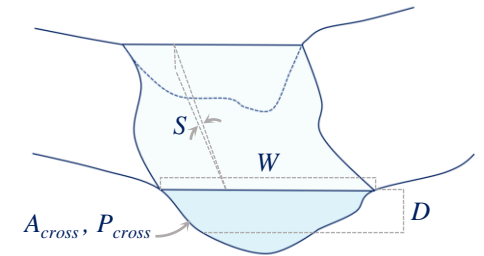
A_{cross} - River Cross-section Area

R - Hydraulic Radius

P_{cross} - River Cross-section Perimeter

S - Water Surface Slope

n - Manning Coefficient of Riverbed Roughness (model parameter)



$$Q = a W^f, Q = b D^g \quad (2) \quad (\text{Gleason \& Smith, 2014})$$

W - Water Surface Width

D - Average Water Depth

a, b, f, g - Parameters

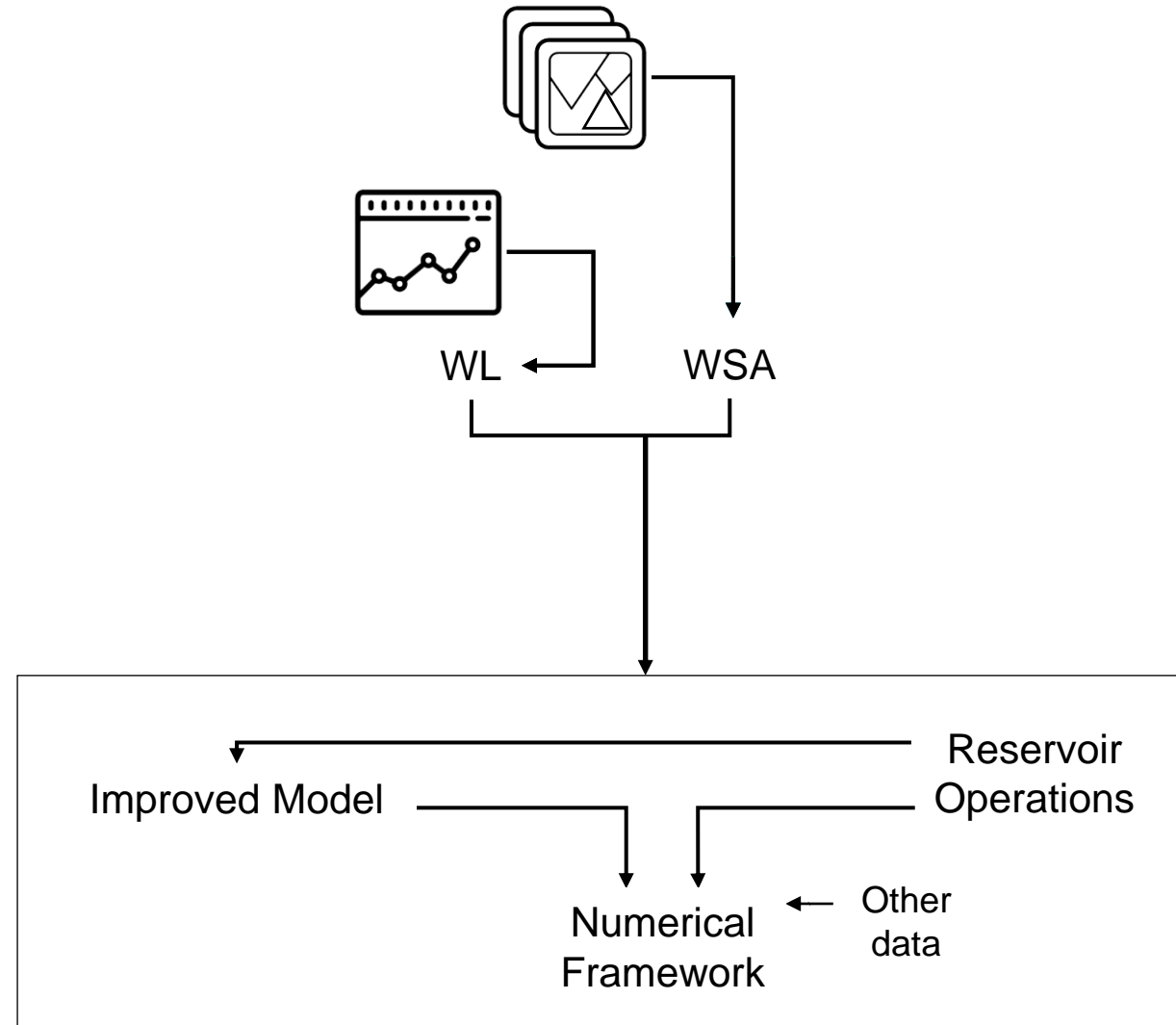
$$Q = c W^h D^i, Q = b D^g \quad (3) \quad (\text{Huang et al., 2020})$$

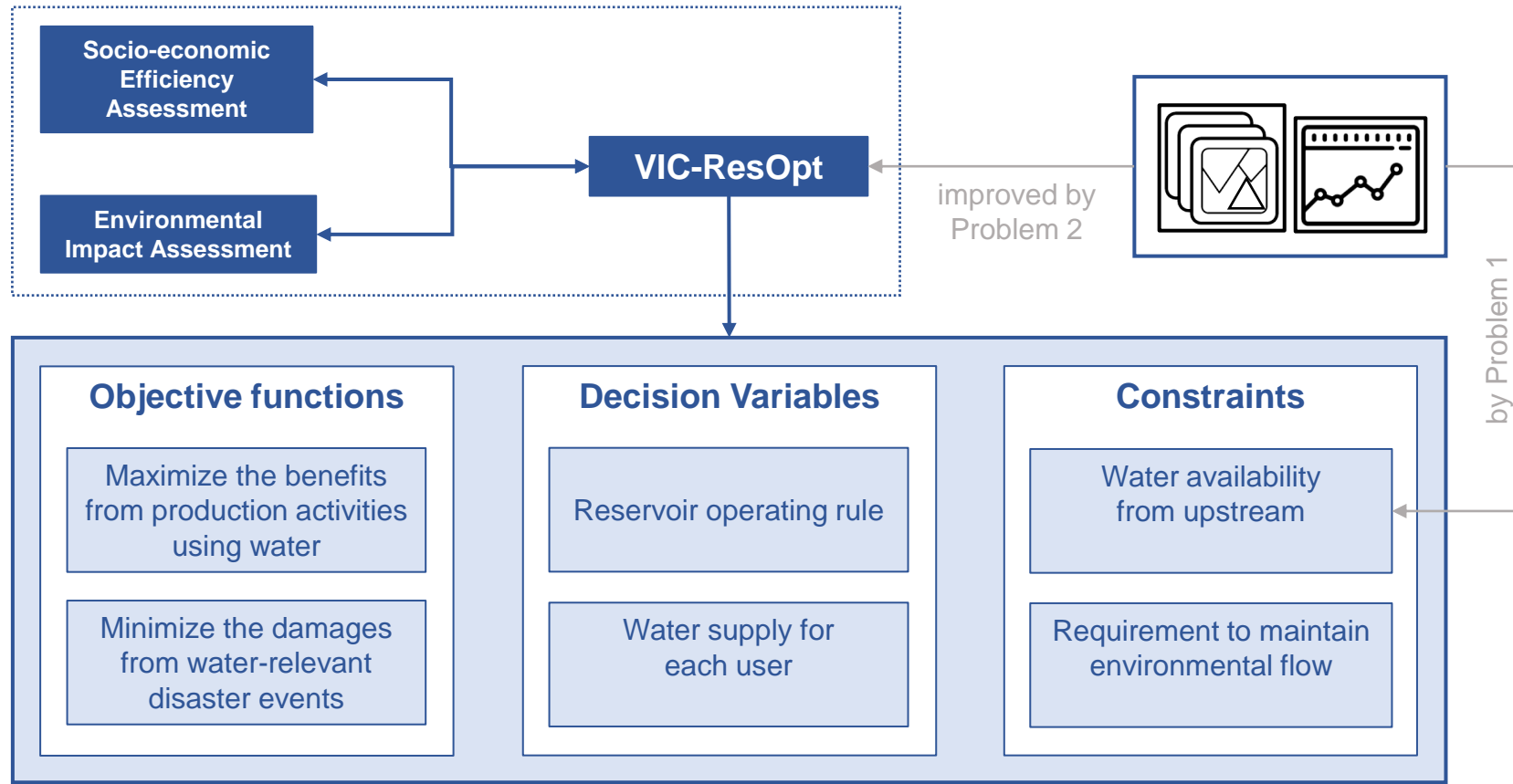
b, c, g, h, i - Parameters

$$Q = e W^j D^k S^l \quad (4) \quad (\text{Bjerklie et al., 2003})$$

e, j, k, l - Parameters

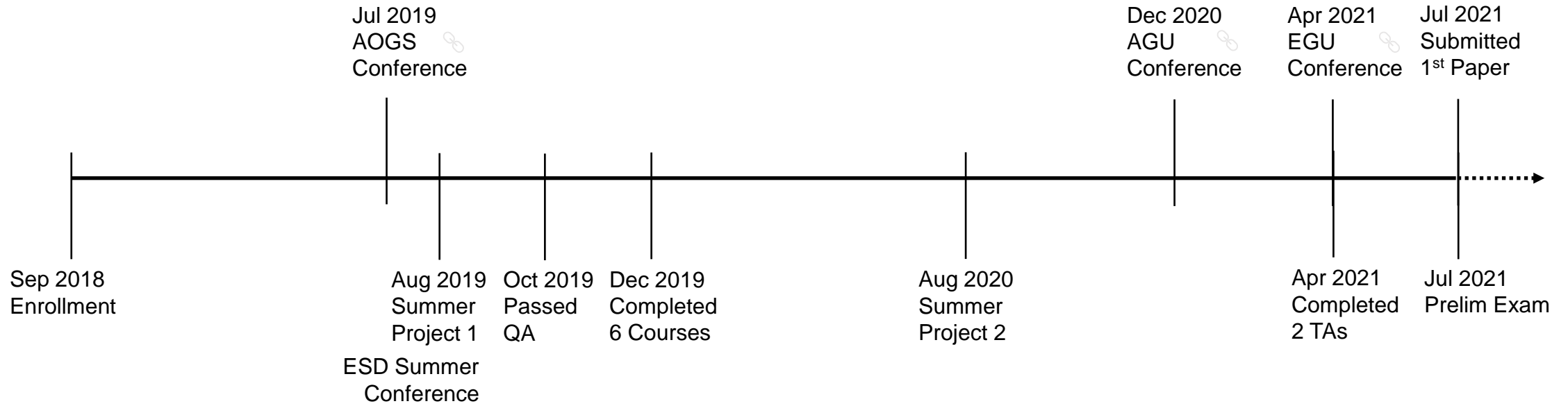
Using **satellite-derived data** to support **downstream countries** in water resources management





Timeline

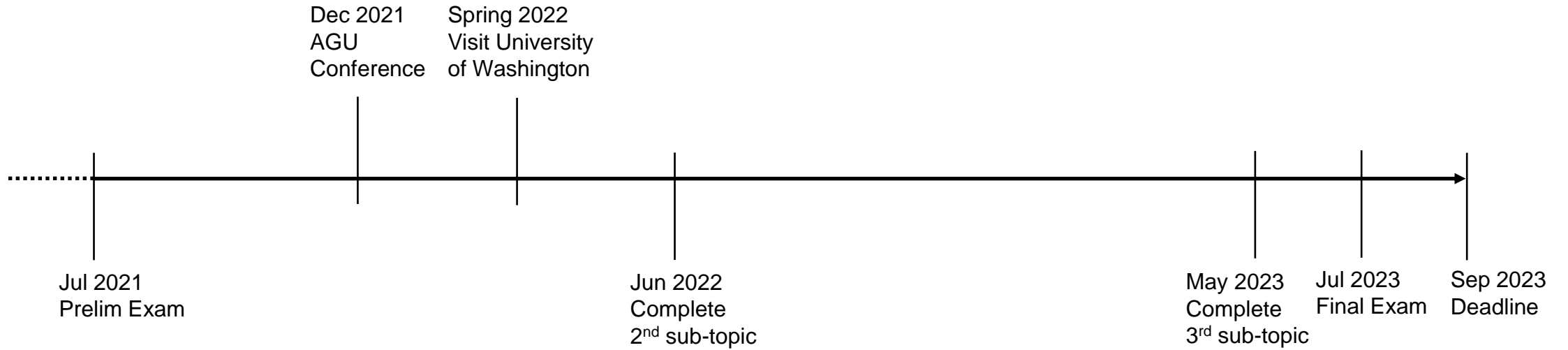
What I have done



AOGS - Asia Oceania Geosciences Society
AGU - American Geophysical Union
EGU - European Geosciences Union

Timeline

What I plan to do



University of Washington

UW Hydro | Computational Hydrology group, Department of Civil and Environmental Engineering - VIC Model Developer

SASWE Research Group, Department of Civil and Environmental Engineering – Remote Sensing and Water Resources Management

References

- Bjerklie, D. M., Dingman, S. L., Vorosmarty, C. J., Bolste, C. H., & Congalton, R. G. (2003). Evaluating the potential for measuring river discharge from space. *Journal of Hydrology*, 278(1-4), 17-38. doi: [10.1016/s0022-1694\(03\)00129-x](https://doi.org/10.1016/s0022-1694(03)00129-x)
- Bonnema, M., & Hossain, F. (2017). Inferring reservoir operating patterns across the Mekong Basin using only space observations. *Water Resources Research*, 53(5), 3791-3810. doi: [10.1002/2016wr019978](https://doi.org/10.1002/2016wr019978)
- Dang, T. D., Chowdhury, A. K., & Galelli, S. (2020). On the representation of water reservoir storage and operations in large-scale hydrological models: Implications on model parameterization and climate change impact assessments. *Hydrology and Earth System Sciences*, 24(1), 397-416. doi: [10.5194/hess-24-397-2020](https://doi.org/10.5194/hess-24-397-2020)
- Dang, T. D., Vu, D. T., Chowdhury, A. K., & Galelli, S. (2020). A software package for the representation and optimization of water reservoir operations in the VIC hydrologic model. *Environmental Modelling & Software*, 126, 104673. doi: [10.1016/j.envsoft.2020.104673](https://doi.org/10.1016/j.envsoft.2020.104673)
- Do, P., Tian, F., Zhu, T., Zohidov, B., Ni, G., Lu, H., & Liu, H. (2020). Exploring synergies in the water-food-energy nexus by using an integrated hydro-economic optimization model for the Lancang-Mekong River Basin. *Science of The Total Environment*, 728, 137996. doi: [10.1016/j.scitotenv.2020.137996](https://doi.org/10.1016/j.scitotenv.2020.137996)
- Döll, P., Berkhoff, K., Bormann, H., Fohrer, N., Gerten, D., Hagemann, S., and Krol, M. (2008). Advances and visions in large-scale hydrological modelling: Findings from the 11th Workshop on Large-Scale Hydrological Modelling. *Advances in Geosciences*, 18, 51-61, doi: [10.5194/adgeo-18-51-2008](https://doi.org/10.5194/adgeo-18-51-2008)
- Duan, Z., & Bastiaanssen, W. G. M. (2013). Estimating water volume variations in lakes and reservoirs from four operational satellite altimetry databases and satellite imagery data. *Remote Sensing of Environment*, 134, 403-416. doi: [10.1016/j.rse.2013.03.010](https://doi.org/10.1016/j.rse.2013.03.010)
- Gao, H., Birkett, C., & Lettenmaier, D. P. (2012). Global monitoring of large reservoir storage from satellite remote sensing. *Water Resources Research*, 48(9), w09504. doi: [10.1029/2012wr012063](https://doi.org/10.1029/2012wr012063)
- Gleason, C. J., & Smith, L. C. (2014). Toward global mapping of river discharge using satellite images and at-many-stations hydraulic geometry. *Proceedings of the National Academy of Sciences of the United States of America*, 111(13), 4788-479. doi: [10.1073/pnas.1317606111](https://doi.org/10.1073/pnas.1317606111)
- Huang, Q., Long, D., Du, M., Han, Z., & Han, P. (2020). Daily continuous river discharge estimation for ungauged basins using a hydrologic model calibrated by satellite altimetry: Implications for the SWOT mission. *Water Resources Research*, 56(7), e2020WR027309. doi: [10.1029/2020wr027309](https://doi.org/10.1029/2020wr027309)

References



- Liu, G., Schwartz, F. W., Tseng, K., & Shum, C. K. (2015). Discharge and water-depth estimates for ungauged rivers: Combining hydrologic, hydraulic, and inverse modeling with stage and water-area measurements from satellites. *Water Resources Research*, 51(8), 6017-6035. doi: [10.1002/2015wr016971](https://doi.org/10.1002/2015wr016971)
- Liu, K.-T., Tseng, K.-H., Shum, C. K., Liu, C.-Y., Kuo, C.-Y., Liu, G., . . . Shang, K. (2016). Assessment of the impact of reservoirs in the Upper Mekong River using satellite radar altimetry and remote sensing imageries. *Remote Sensing*, 8(5), 367. doi: [10.3390/rs8050367](https://doi.org/10.3390/rs8050367)
- Markert, K. N., Pulla, S. T., Lee, H., Markert, A. M., Anderson, E. R., Okeowo, M. A., & Limaye, A. S. (2019). AltEx: An open source web application and toolkit for accessing and exploring altimetry datasets. *Environmental Modelling & Software*, 117, 164-175, doi: [10.1016/j.envsoft.2019.03.021](https://doi.org/10.1016/j.envsoft.2019.03.021)
- McCracken, M. & Wolf, A. T. (2019). Updating the Register of International River Basins of the world. *International Journal of Water Resources Development*, 35, 732–782. doi: [10.1080/07900627.2019.1572497](https://doi.org/10.1080/07900627.2019.1572497)
- Pekel, J.-F., Cottam, A., Gorelick, N., & Belward, A. S. (2016). High-resolution mapping of global surface water and its long-term changes. *Nature*, 540, 418-422. doi: [10.1038/nature20584](https://doi.org/10.1038/nature20584)
- Tang, Q., Oki, T., Kanae, S. (2006). A distributed biosphere hydrological model (DBHM) for large river basin, *Proceedings of Hydraulic Engineering*, 50, 37-42. doi: [10.2208/prohe.50.37](https://doi.org/10.2208/prohe.50.37)
- Turner, S. W. D., Doering, K., & Voisin, N. (2020). Data-driven reservoir simulation in a large-scale hydrological and water resource model. *Water Resources Research*, 56(10), e2020wr027902. doi: [10.1029/2020wr027902](https://doi.org/10.1029/2020wr027902)
- Wolf, A. T., Kramer, A., Carius, A., & Dabelko, G. D. (2005) *State of the World 2005: Redefining global security*. Newyork: W. W. Norton & Company
- Zhang, S., Gao, H., & Naz, B. S. (2014). Monitoring reservoir storage in South Asia from multisatellite remote sensing. *Water Resources Research*, 50(11), 8927-8943. doi: [10.1002/2014wr015829](https://doi.org/10.1002/2014wr015829)
- Zhai, K., Wu, X., Qin, Y., & Du, P. (2015). Comparison of surface water extraction performances of different classic water indices using OLI and TM imageries in different situations. *Geospatial Information Science*, 18(1), 34-42. doi: [10.1080/10095020.2015.1017911](https://doi.org/10.1080/10095020.2015.1017911)

APPENDICES

Example of International Water Agreement

Atlas of International Freshwater Agreements, 2002, UNEP

Date	Treaty Basin	Signatories	Treaty Name
April 30, 1973	Colorado	Mexico; United States of America	Agreement extending Minute No. 241 of the International Boundary and Water Commission, United States and Mexico, on July 14, 1972, as extended
July 14, 1972	Colorado	Mexico; United States of America	Agreement effected by Minute No. 241 of the International Boundary and Water Commission, United States and Mexico, adopted at El Paso
August 24, 1966	Colorado	Mexico; United States of America	Exchange of notes constituting an agreement concerning the loan of waters of the Colorado River for irrigation of lands in the Mexicali Valley
November 14, 1944	Colorado, Rio Bravo del Norte, Rio Grande, Tijuana	Mexico; United States of America	Treaty between the United States of America and Mexico relating to the waters of the Colorado and Tijuana Rivers, and of the Rio Grande (Rio Bravo) from Fort Quitman, Texas, to the Gulf of Mexico, signed at Washington on February 3, 1944, and supplementary protocol, signed at Washington on November 14, 1944
November 21, 1900	Colorado, Rio Grande	Mexico; United States of America	Boundary waters: Rio Grande and Rio Colorado, November 21, 1900, extension of convention of March 1, 1889
December 22, 1899	Colorado, Rio Grande	Mexico; United States of America	Boundary waters: Rio Grande and Rio Colorado, December 22, 1899, extension of convention of March 1, 1889
December 2, 1898	Colorado, Rio Grande	Mexico; United States of America	Boundary waters: Rio Grande and Rio Colorado, December 2, 1898, extension of convention of March 1, 1889
October 29, 1897	Colorado, Rio Grande	Mexico; United States of America	Boundary waters: Rio Grande and Rio Colorado, October 29, 1897, extension of convention of March 1, 1889
November 6, 1896	Colorado, Rio Grande	Mexico; United States of America	Boundary waters: Rio Grande and Rio Colorado, November 6, 1896, extension of convention of March 1, 1889
October 1, 1895	Colorado, Rio Grande	Mexico; United States of America	Boundary waters: Rio Grande and Rio Colorado, October 1, 1895, extension of convention of March 1, 1889
March 1, 1889	Colorado, Rio Grande	Mexico; United States of America	Convention on boundary waters: Rio Grande and Rio Colorado

Colorado

Total area: 655,000 km²

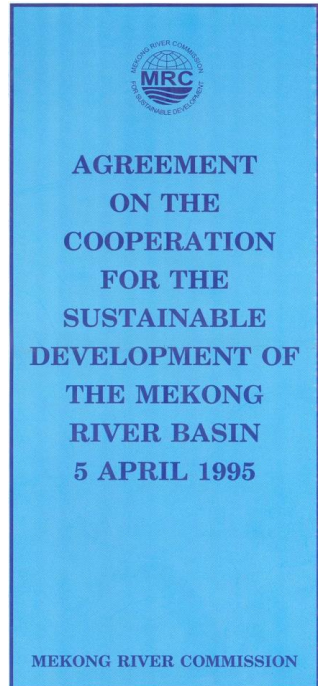
Countries	Area of Basin in Country km ²	%
United States of America	644,600	98.41
Mexico	10,400	1.59



Date	Treaty Basin	Signatories	Treaty Name
July 16, 1994	Colorado	United Mexican States; United States of America	Minute No. 291 of the International Boundary and Water Commission, U.S.A. and Mexico, concerning improvements to the conveying capacity of the international boundary segment of the Colorado River
July 18, 1985	Frontier or shared waters	United Mexican States; United States of America	Agreement of cooperation between the United States of America and the United Mexican States regarding pollution of the environment along the inland international boundary by discharges of hazardous substances
August 14, 1983	Frontier or shared waters	United Mexican States; United States of America	Agreement between the United States of America and the United Mexican States on cooperation for the protection and improvement of the environment in the border area
August 30, 1973	Colorado	United Mexican States; United States of America	Mexico-US agreement on the permanent and definitive solution to the salinity of the Colorado River Basin (International Boundary and Water Commission Minute No. 242)

Example of International Water Agreement

Atlas of International Freshwater Agreements, 2002, UNEP



For The Kingdom of Cambodia:


Ing Kieth

Deputy Prime Minister and
Minister of Public Works and Transport

For The Lao People's Democratic Republic:


Somsavat Lengsavad

Minister of Foreign Affairs


For the Kingdom of Thailand:


Krasae Chanawongse

Minister of Foreign Affairs

For the Socialist Republic of
Viet Nam:


Nguyen Manh Cam
Ministry of Foreign Affairs



42 Articles

Article 6. Maintenance of Flows on the Mainstream

To cooperate in the maintenance of the flows on the mainstream from diversions, storage releases, or other actions of a permanent nature; except in the cases of historically severe droughts and/or floods:

- A. Of not less than the acceptable minimum monthly natural flow during each month of the dry season;

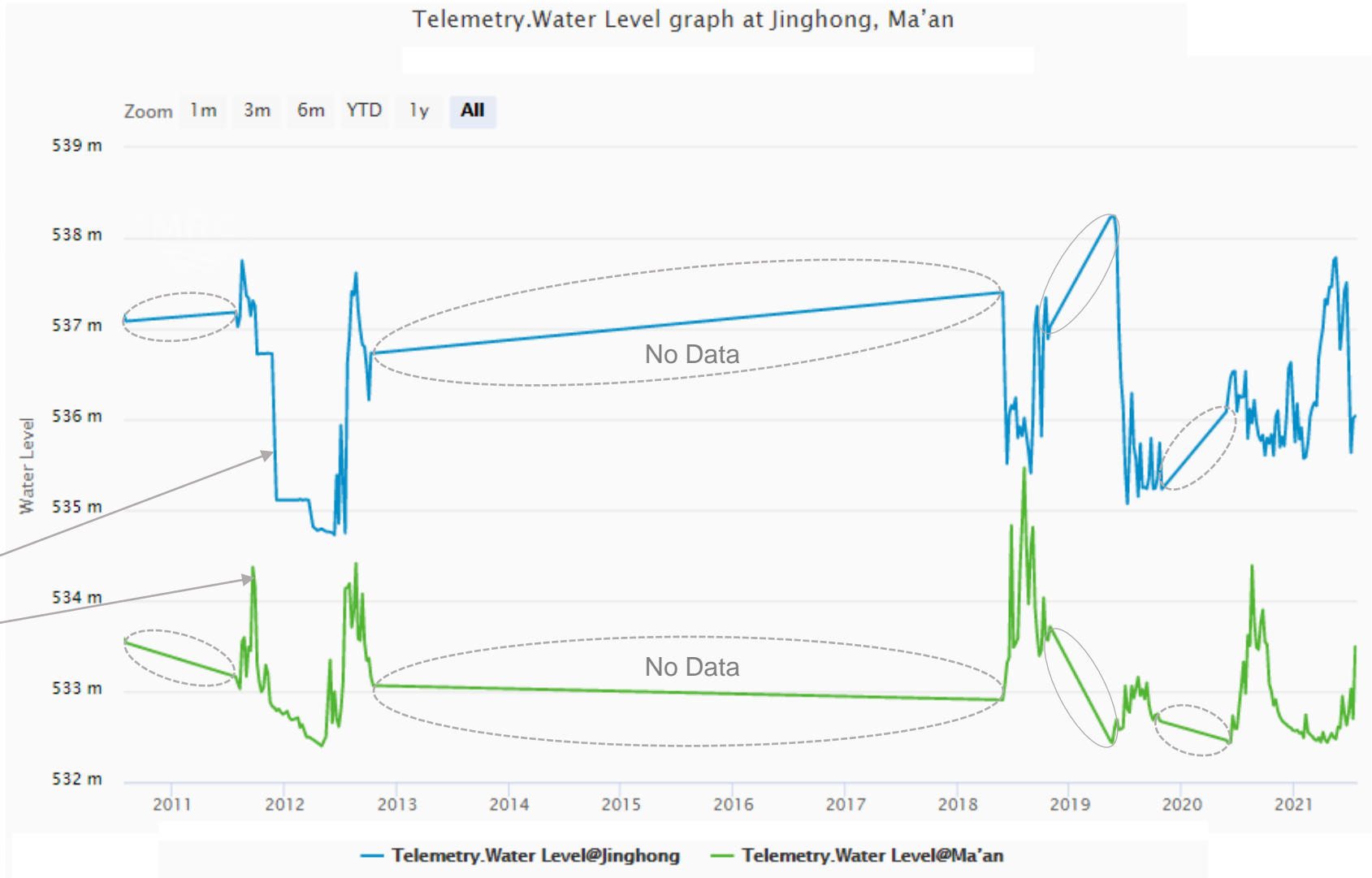
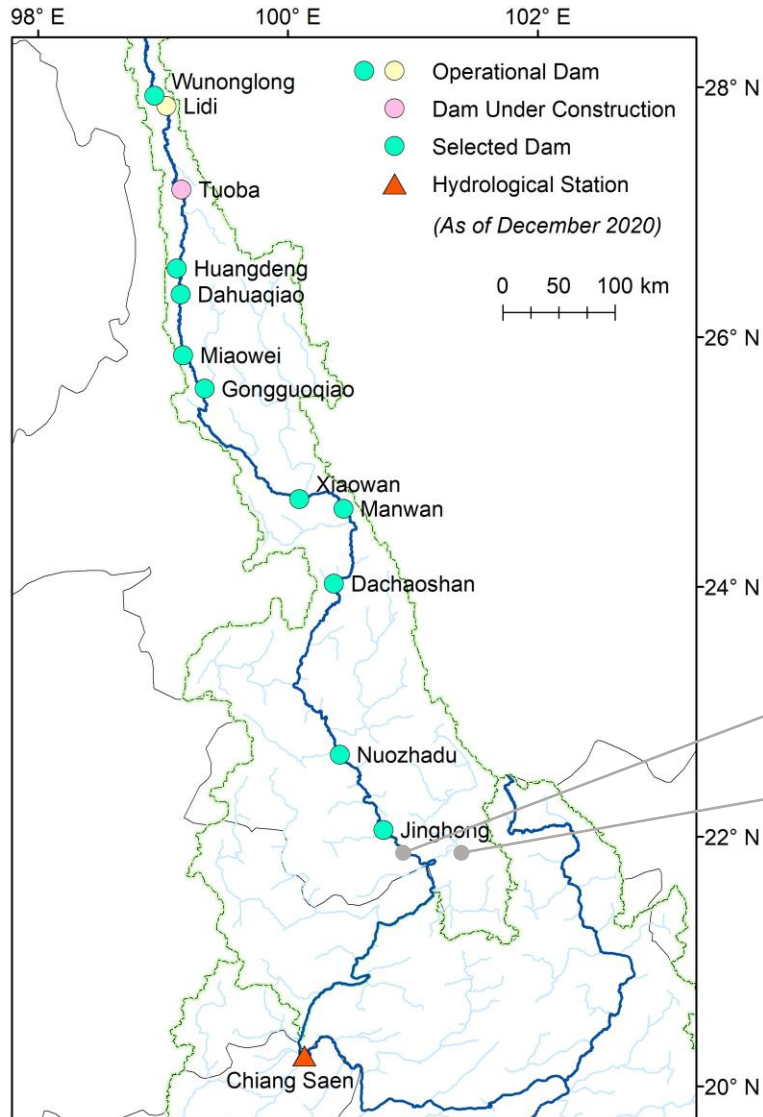
Mekong*

Total area: 787,800 km²

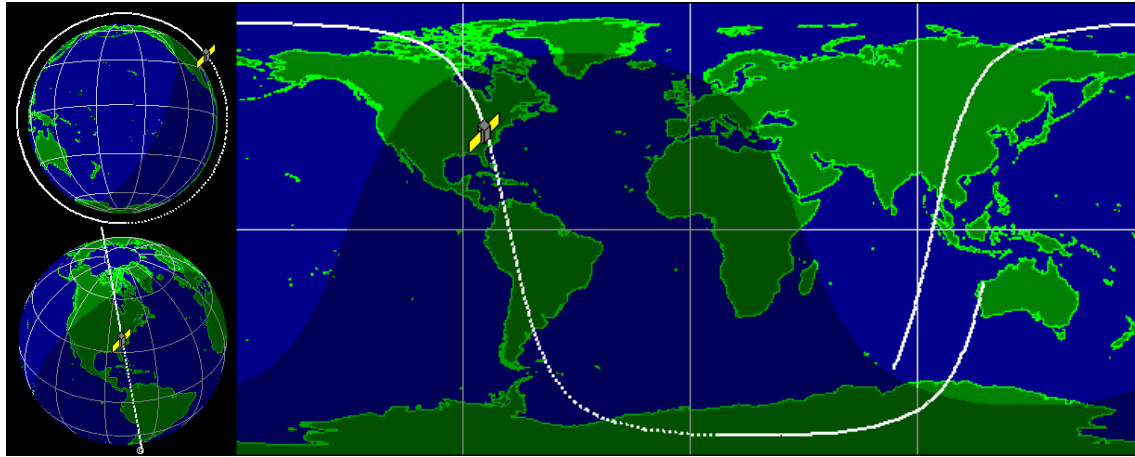
Countries	Area of Basin in Country km ²	%
Laos, People's Democratic Republic of	198,000	25.14
Thailand	193,900	24.62
China	171,700	21.79
Cambodia (Kampuchea)	158,400	20.10
Vietnam	38,200	4.84
Myanmar (Burma)	27,600	3.51



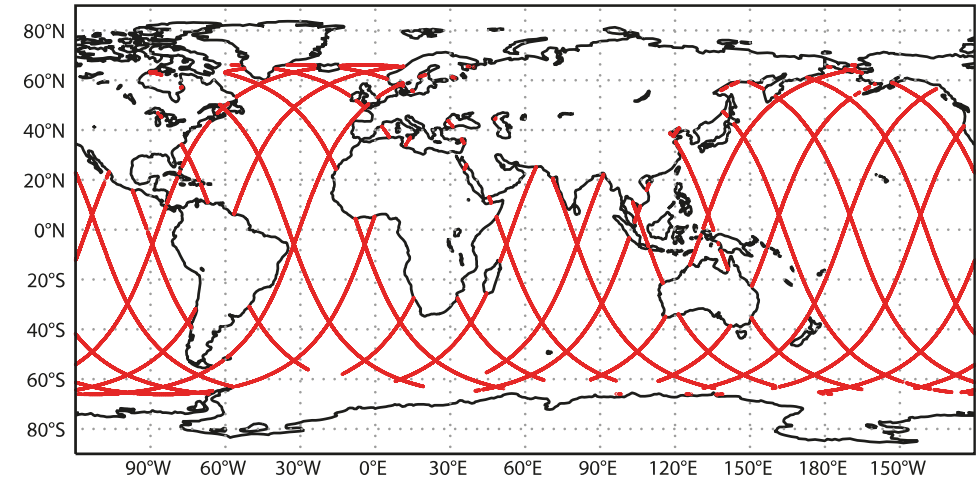
Date	Treaty Basin	Signatories	Treaty Name
April 5, 1995	Mekong	Cambodia; Laos, People's Democratic Republic; Thailand; Vietnam, Socialist Republic of	Agreement on the cooperation for the sustainable development of the Mekong River Basin
January 5, 1978	Mekong	Laos, People's Democratic Republic; Thailand; Vietnam, Socialist Republic of	Declaration concerning the Interim Committee for Coordination of Investigation of the Lower Mekong Basin
January 31, 1975	Mekong	Khmer, Republic of; Laos; Thailand; Vietnam	Joint declaration of principles for utilization of the waters of the lower Mekong Basin, signed by the representatives of the governments of Cambodia, Laos, Thailand, and Vietnam to the Committee for Coordination of Investigations of the Lower Mekong Basin
August 12, 1965	Mekong, Nam Ngum, Nam Pong	Laos; Thailand	Convention between Laos and Thailand for the supply of power
October 31, 1957	Mekong	Cambodia; Laos; Thailand; Vietnam, Republic of	Statute of the Committee for Coordination of Investigations of the Lower Mekong Basin established by the governments of Cambodia, Laos, Thailand, and the Republic of Viet-Nam in response to the decisions taken by the United Nations Economic Commission for Asia and the Far East



Satellite Imagery and Altimetry Data Collection

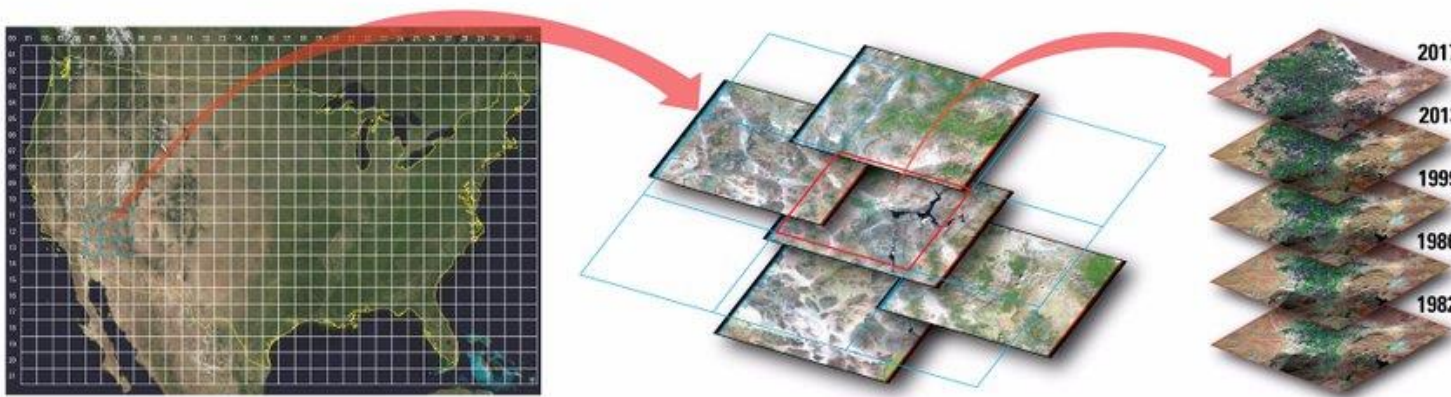


Landsat orbit (views from above orbit plan and above satellite) and ground track
 Images adapted from heavens-above.com



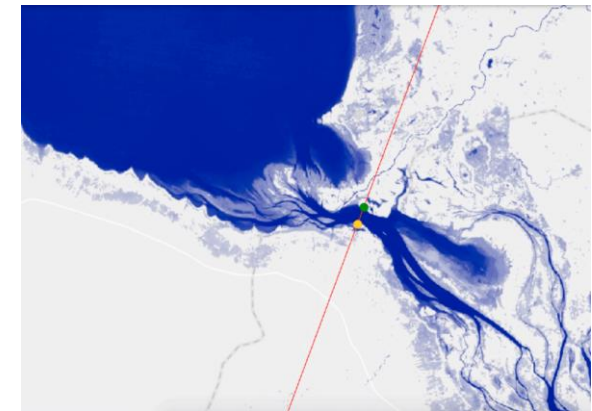
Janson ground track

Images adapted from the *Use of Radar Altimeter Products* by the European Centre for Medium-Range Weather Forecasts (ECMWF), 2016



Landsat image tiles and their global coverage

Images adapted from United States Geological Survey (USGS)



Jason Altimetry is only available for the water bodies with > 350m width along the satellite ground track

Images adapted from [Markert et al. \(2019\)](#)

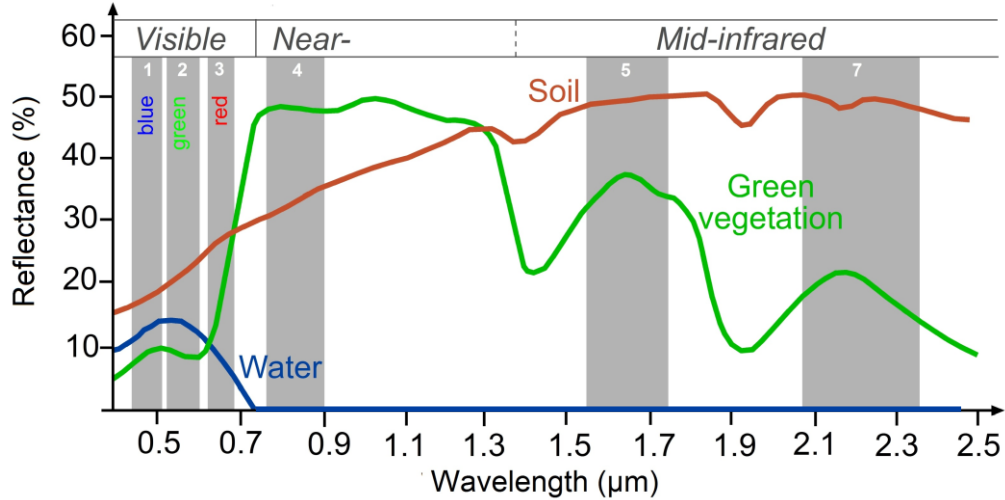
Landsat Image

Wavelength and ID of some bands of Landsat 5, 7, and 8 images

Band	Wavelength (micrometer)	Landsat 5, 7	Landsat 8
Blue	0.43 - 0.45	1	2
Green	0.45 - 0.51	2	3
Red	0.53 - 0.59	3	4
Near Infrared (NIR)	0.64 - 0.67	4	5
Quality Assessment		BQA	BQA

Spectral indices for water surface extraction

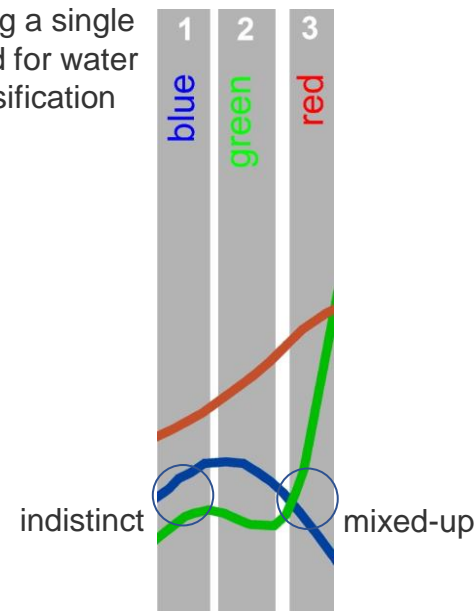
Index	Formula	Recommended Threshold Value
NDVI (Normalized Difference Vegetation Index)	Red-Green	0 (Zhai et al., 2015)
	Red+Green	0.1 (Gao et al., 2012)
NDWI (Normalized Difference Water Index)	Green-NIR	0 (Zhai et al., 2015),
	Green+NIR	0 (Bonnema & Hossain, 2017)
MNDWI (Modified Normalized Difference Water Index)	Green-MIR	0 and 0.1
	Green+MIR	(Duan & Bastiaanssen, 2013)



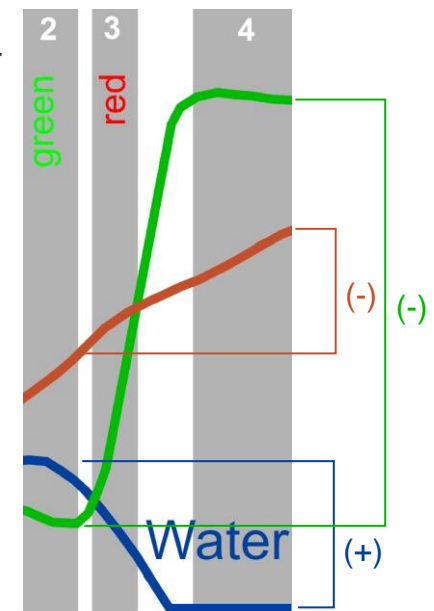
Reflectance of water, soil and vegetation in different wavelengths

Image adapted from [Classification Algorithms and Methods](http://seos-project.eu/classification/classification-c01-p05.html),
seos-project.eu/classification/classification-c01-p05.html

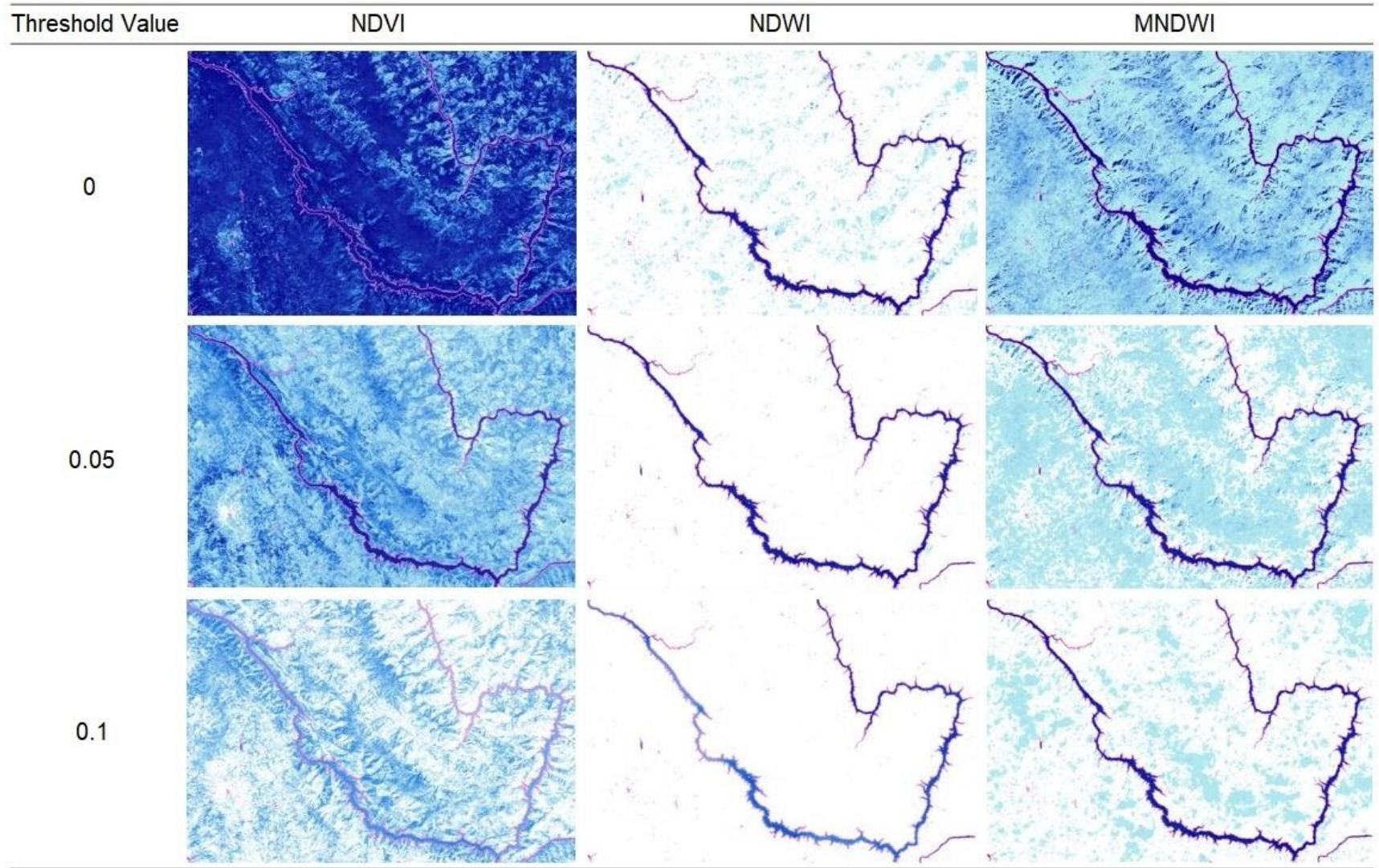
Using a single band for water classification



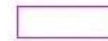
Using multiple bands for water classification



Performance of 3 spectral indices in extracting the water surface area (Xiaowan Reservoir)

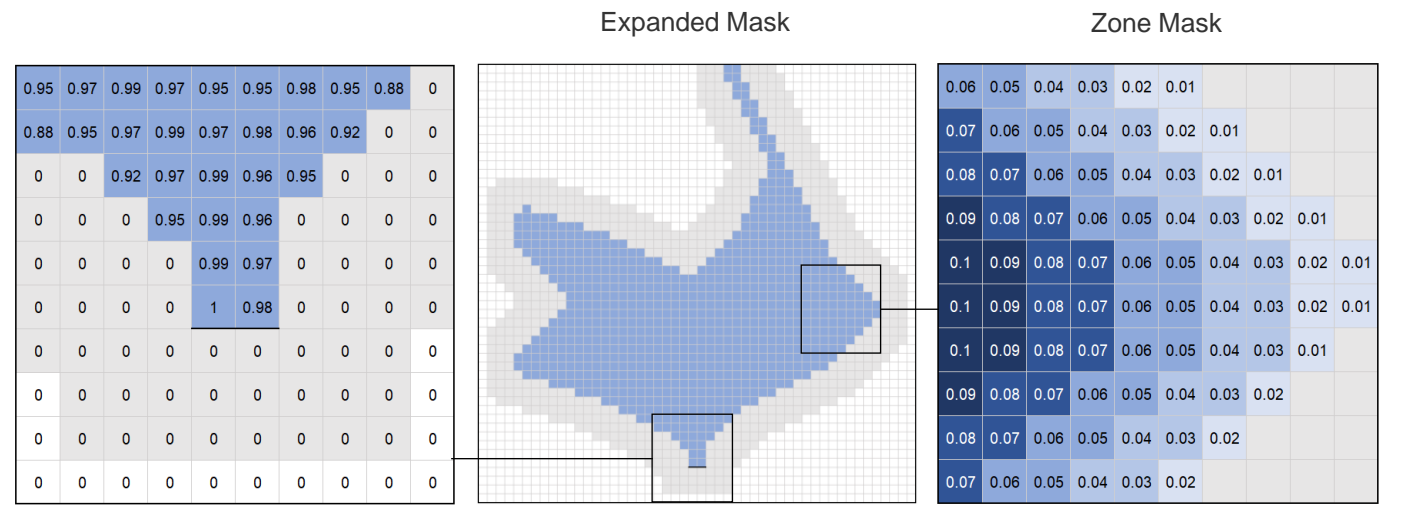
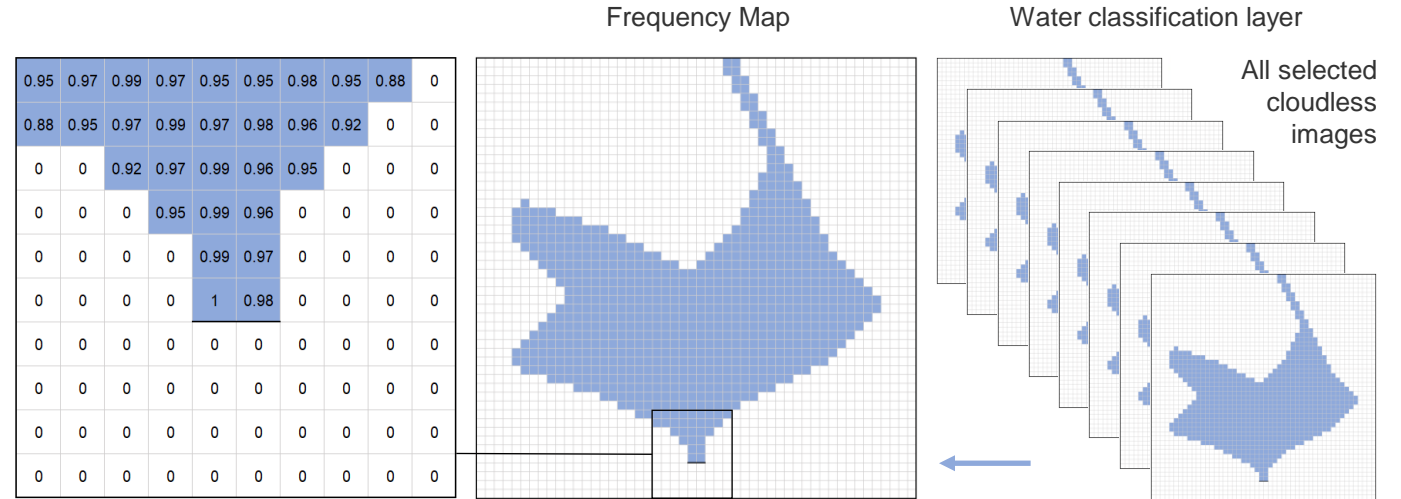
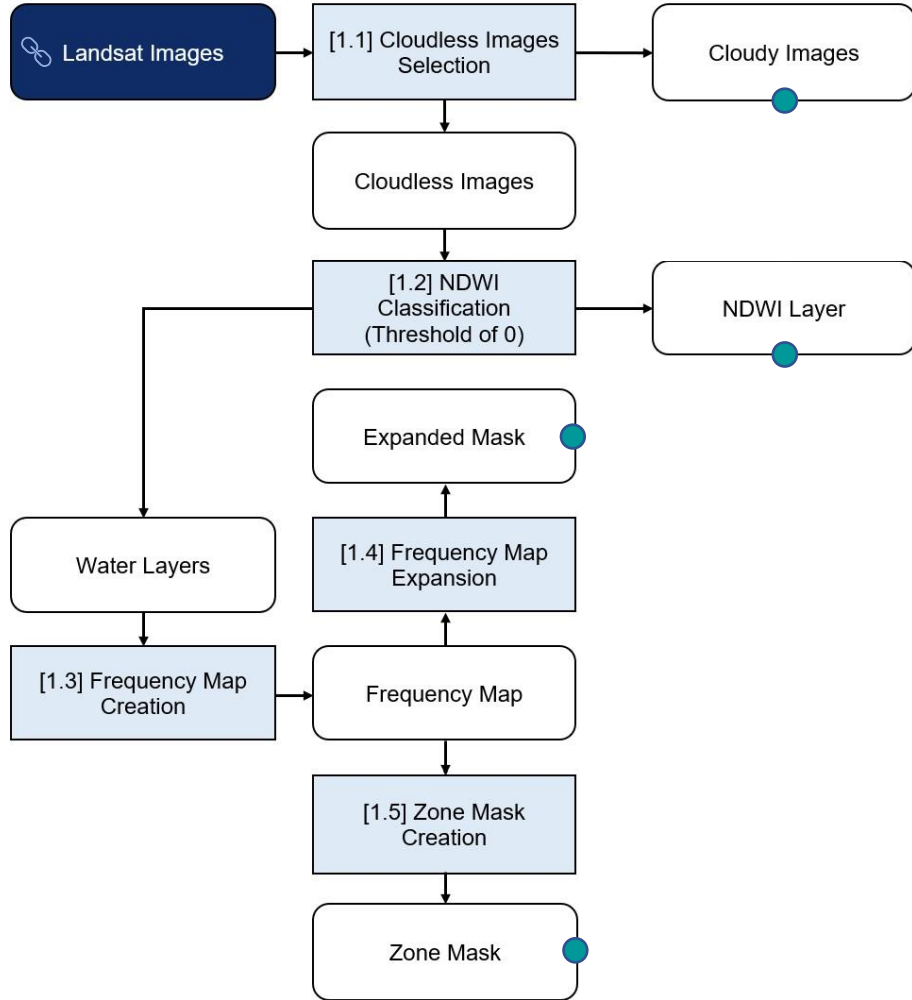


Number of time the pixel being classified as water



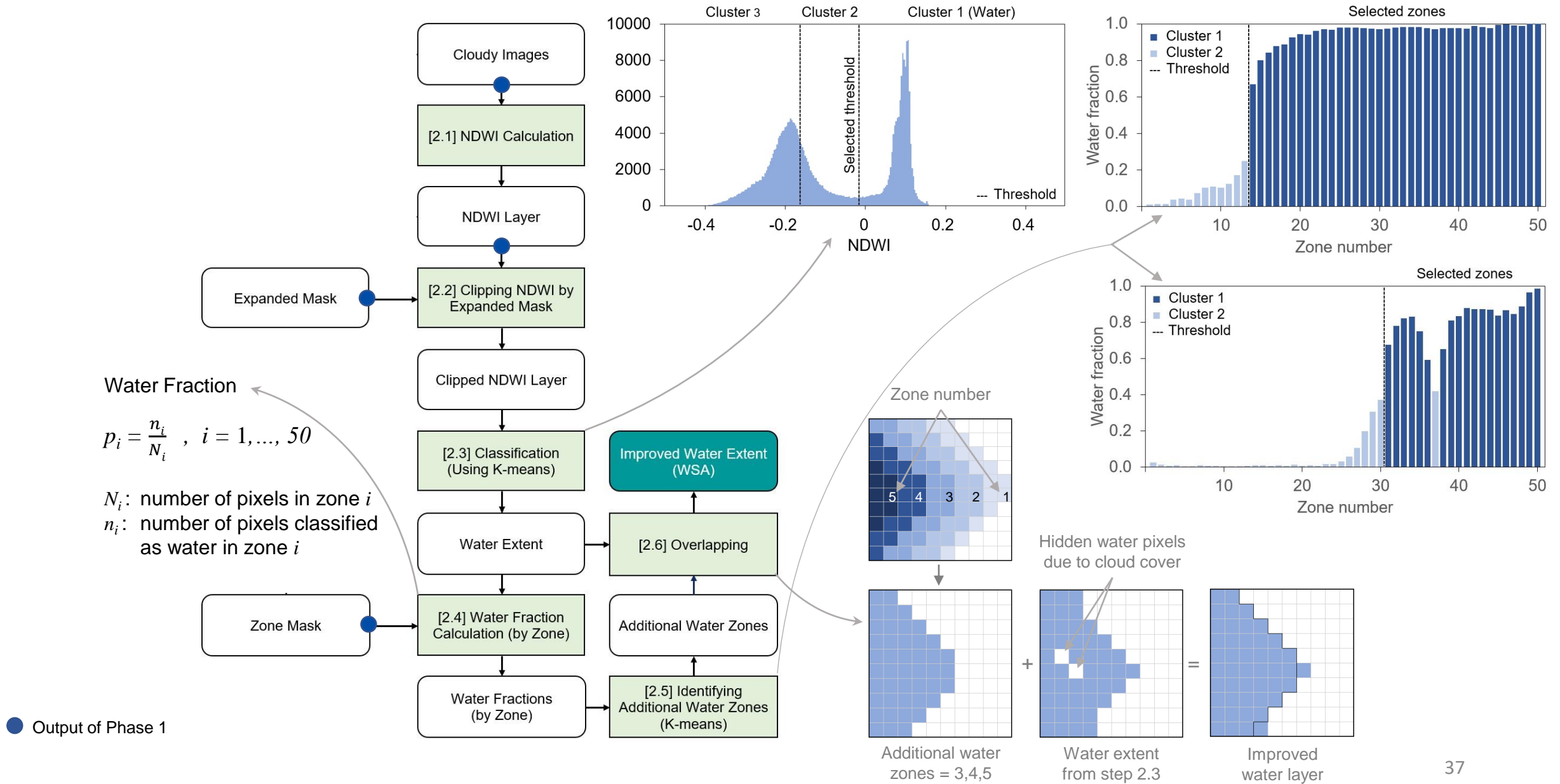
Maximum Water Extent by European Commission's Joint Research Centre (Pekel et al., 2016)

WSA Estimation Algorithm Phase 1

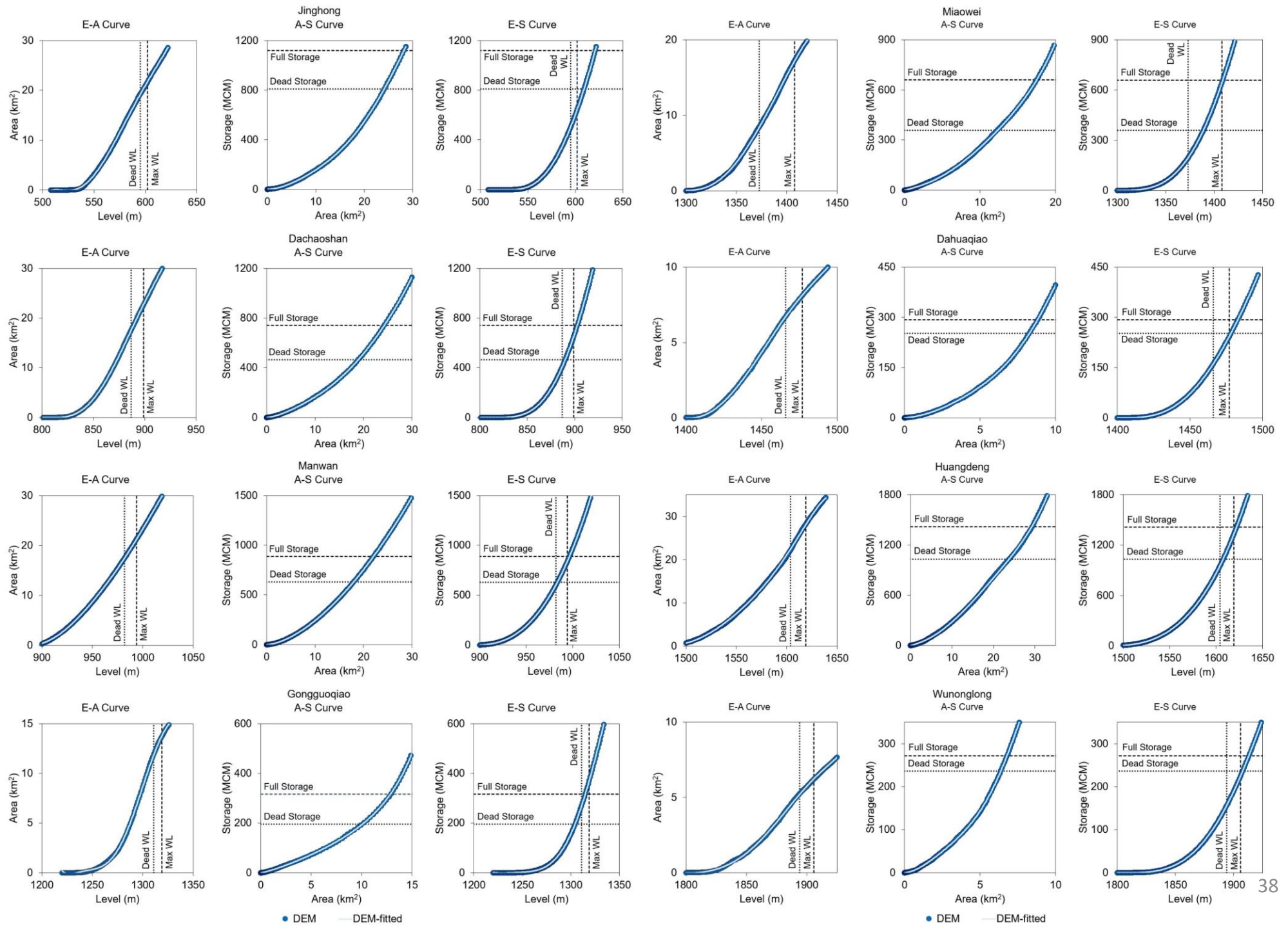


● Input for Phase 2

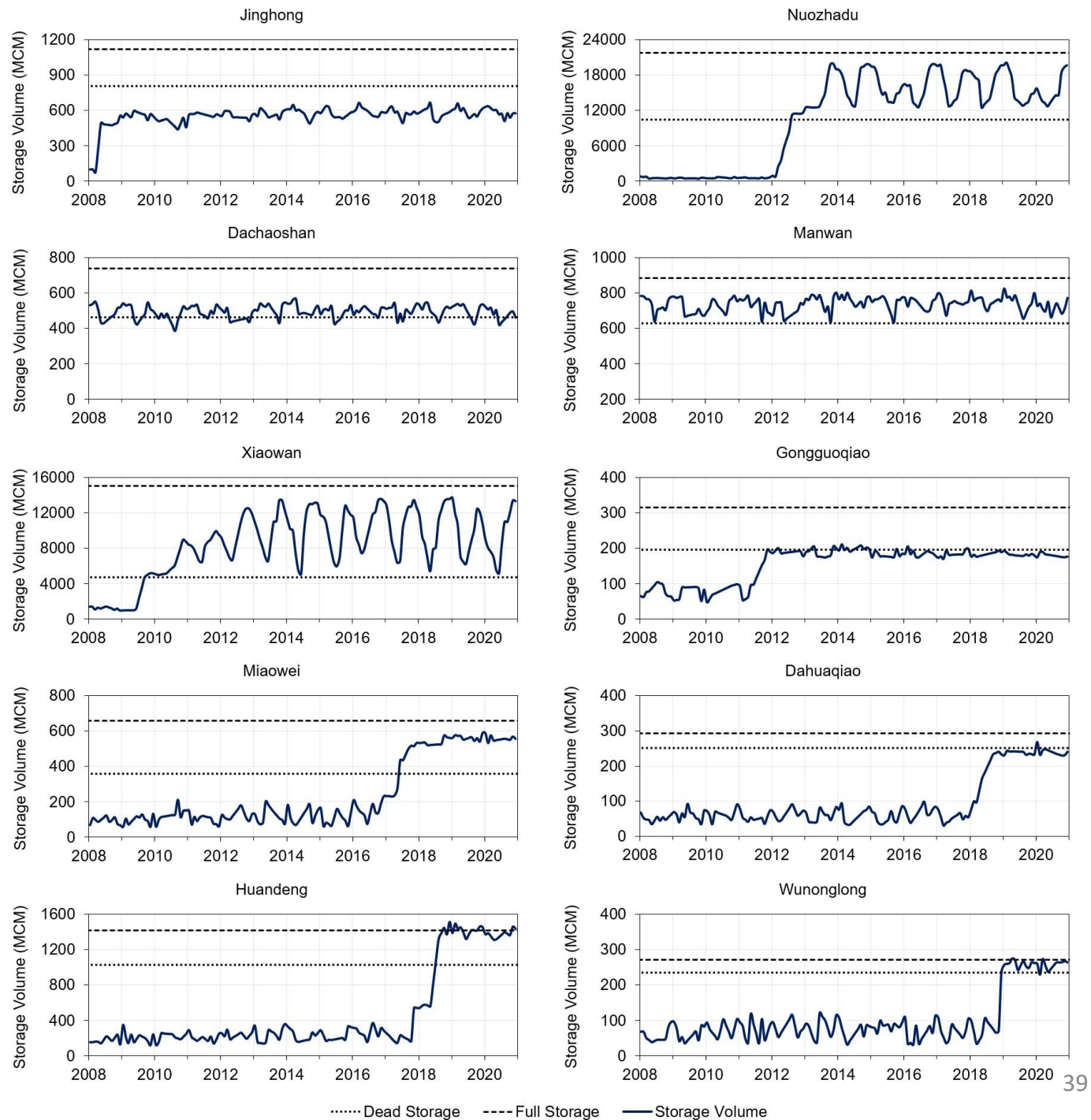
WSA Estimation Algorithm Phase 2



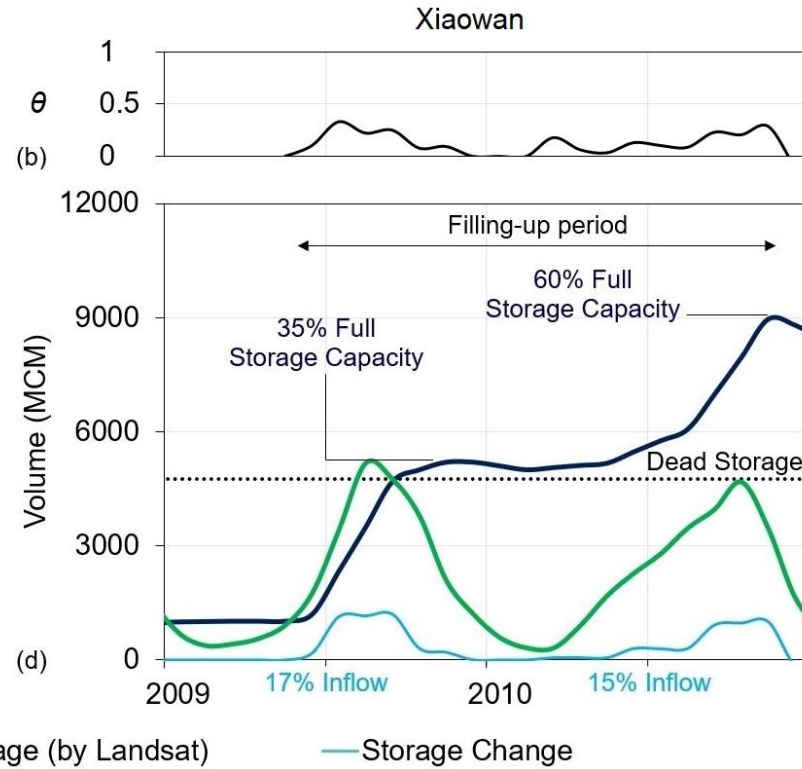
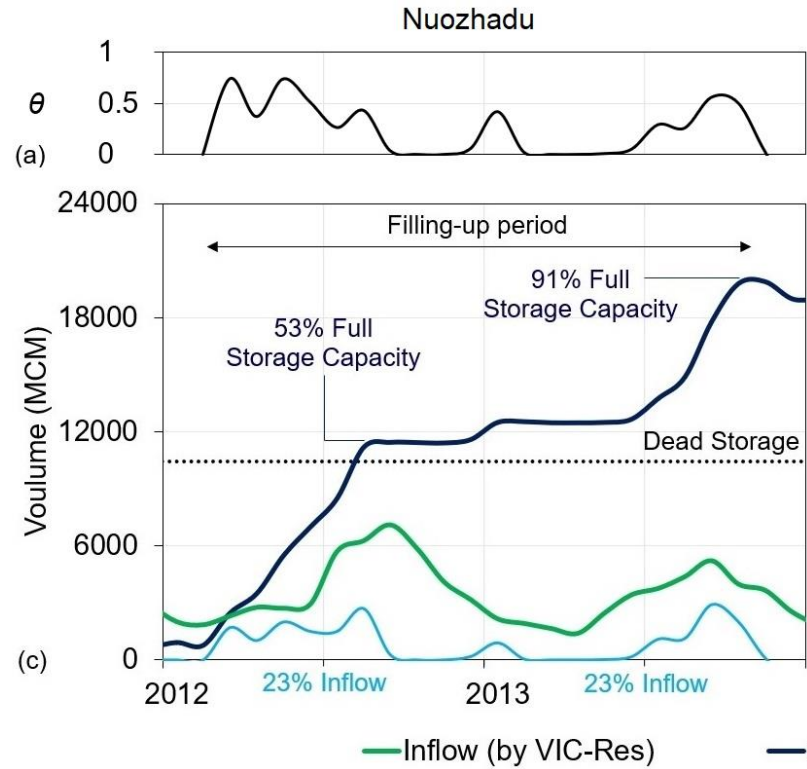
E-A, A-S, and E-S Curves of 8 Reservoirs in the Lancang River



Storage Variation of Individual Reservoirs in the Lancang River



Fraction of inflow retained in reservoirs

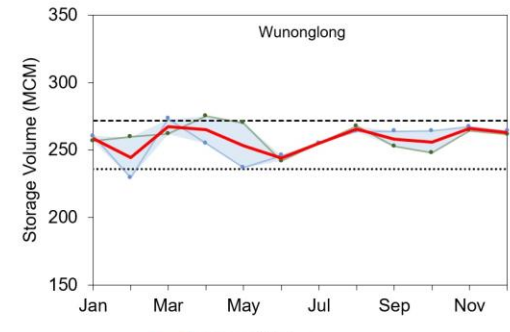
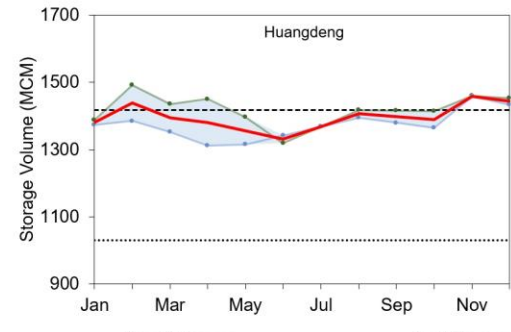
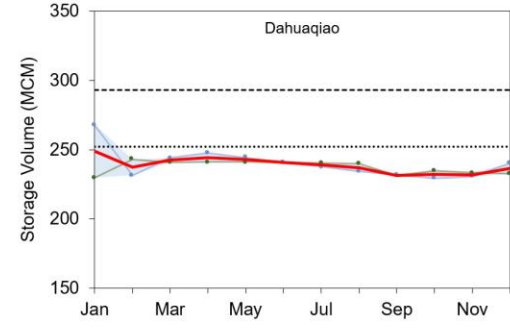
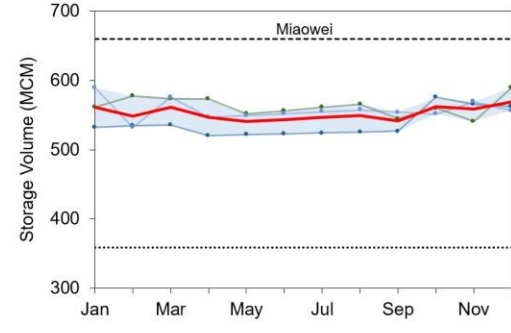
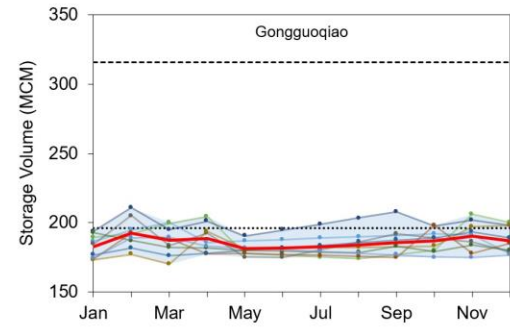
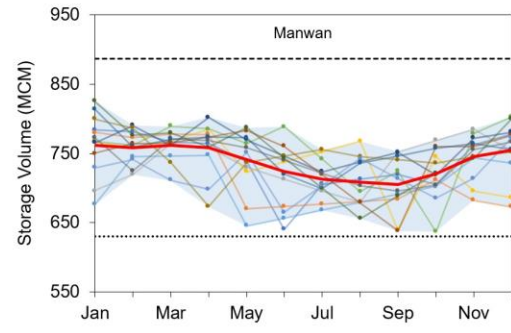
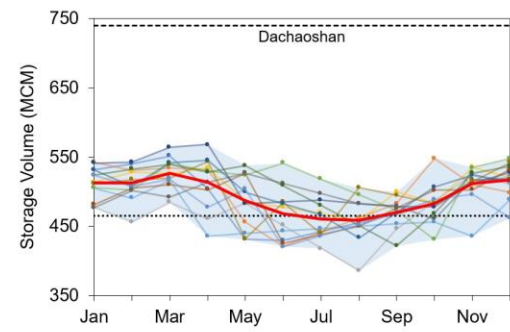
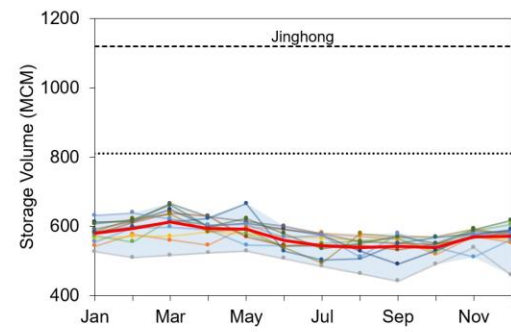


Mass balance equation:

$$S_t = S_{t-1} + \theta Q_t - E_t$$

- S_t - reservoir storage at time t
- Q_t - the inflow volume in the interval $(t-1; t]$
- E_t - the evaporation loss in the interval $(t-1; t]$
- θ - parameter varying between 0 and 1 and expressing the fraction of inflow retained by the reservoir

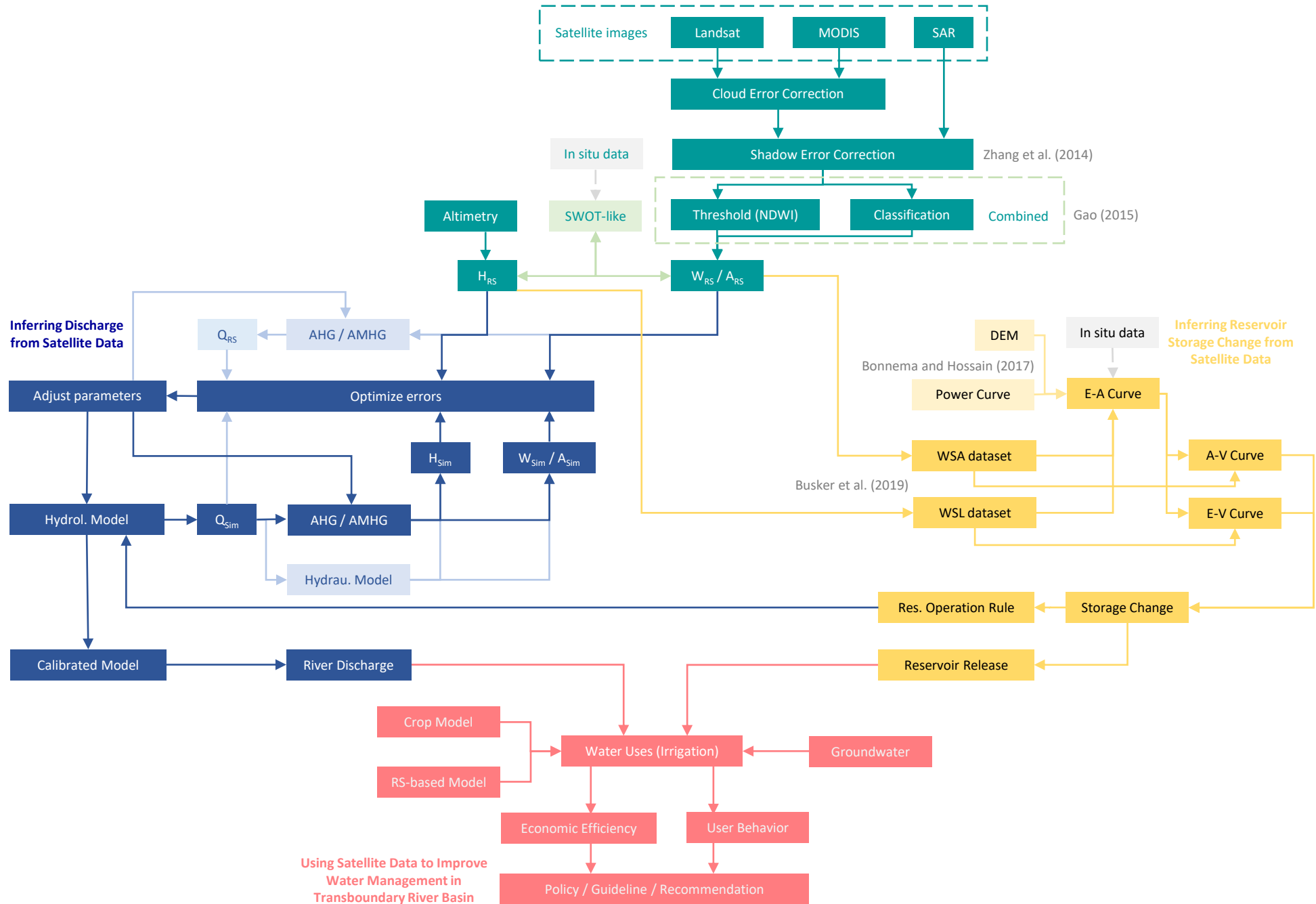
Operation Curves of 8 Reservoirs in the Lancang River



..... Dead Storage --- Full Storage
 2008 2009 2010 2011 2012 2013 2014
 2015 2016 2017 2018 2019 2020
 — Average Storage

Mind Map

July 2020

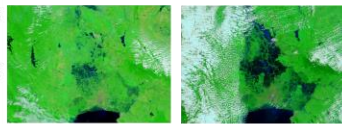
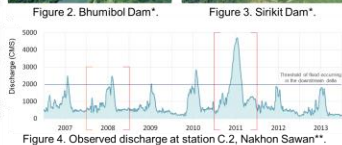
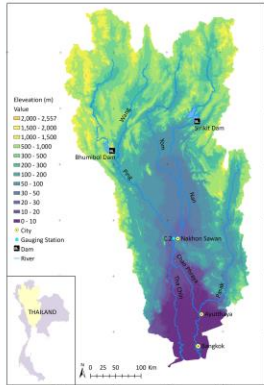


1. PROBLEM STATEMENT AND STUDY SITE

The Chao Phraya Basin is the biggest and most important river basin in Thailand. Four tributaries of the Chao Phraya—Ping, Wang, Yom, and Nan—originate from the mountains in the Northern part of the country, and then merge into the main river that flows through the central area of Thailand—including Bangkok—before pouring into the Gulf of Thailand.

The two largest dams, Bhumibol and Sirikit, were constructed on the Ping and Nan Rivers with the initial purposes of irrigation water supply and hydropower generation. These dams, however, could alter significantly not only the flow regimes, but also the timing, duration, depth, and inundation area of the downstream floods in the Chao Phraya delta.

The historical flood events in Chao Phraya River Basin, especially the 2011 flood, which caused unprecedented economic damages, raised questions on whether this existing reservoir system can be utilized to reduce flood damages in the delta without reducing hydropower production and increasing the irrigation water deficit.



Research Questions

1. Is there an operating policy that strikes a better balance between water supply, hydropower production, and flood mitigation?
2. How do alternative operating policies affect the flood discharge and the timing, duration, depth, and inundation area of the downstream floods?

Source: (*) Electricity Generating Authority of Thailand, (**) Thailand Royal Irrigation Department, (***) NASA

2. METHODOLOGY

A hydrological model, namely the Variable Infiltration Capacity (VIC) model, was implemented for the Chao Phraya Basin to simulate rainfall-runoff processes and streamflow routing. First, we calibrated the main soil parameters of the model using a simulation-optimization approach (see the first blue box in the figure below). Then, we designed alternative operating policies (rule curves) by coupling VIC with a Multi-Objective Evolutionary Algorithm (MOEA).

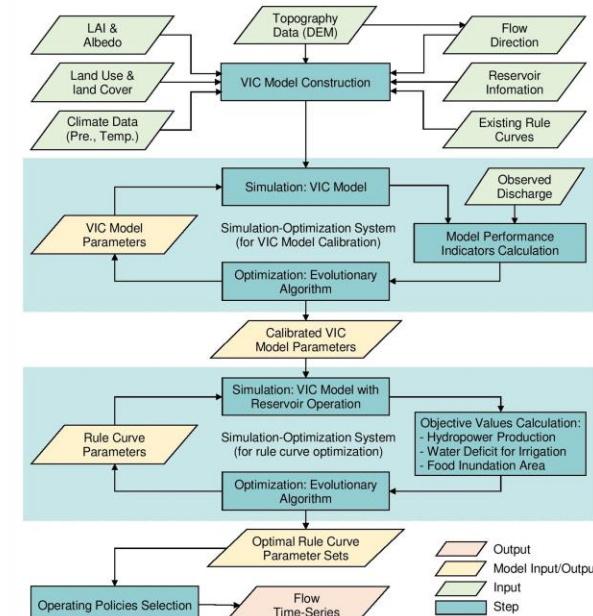


Figure 6. Flowchart representing the adopted methodology.

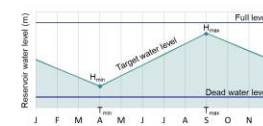
Objectives (for the optimization of the rule curves):

- Average annual food inundation area (to be min.)
- Average annual hydropower production (to be max.)
- Average annual irrigation water deficit (to be min.)

Decision variables:

Rule curve parameters: - H_{min} , H_{max}
- T_{min} , T_{max}

Simulation horizon: 2009-2013



3. PRELIMINARY RESULTS

Pareto frontier

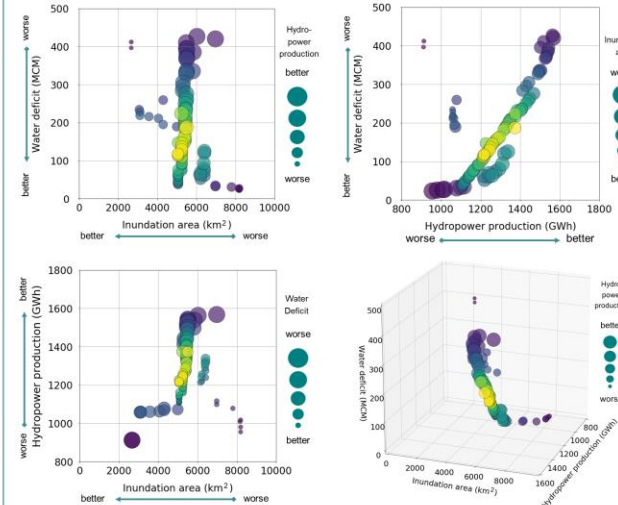


Figure 7. 3D representation of the Pareto frontier (bottom right) and 2D images of the front.

Performance of a selected rule curve

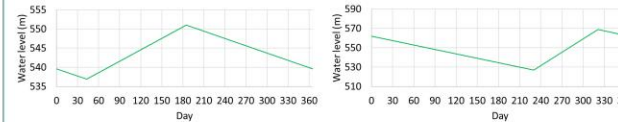


Figure 8. Selected optimal rule curve for Bhumibol (left) and Sirikit (right) reservoir.

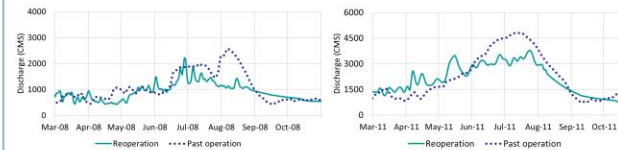


Figure 9. Simulated discharge at station C.2 under the selected optimal rule curve for the 2008 (left) and 2011 floods (right).

4. FUTURE RESEARCH

- A hydrodynamic model, HEC-RAS 2D will be developed for the Chao Phraya delta to simulate the flood inundation in the delta under different operating policies.
- The impacts of climate change may be included in future research.

ESD
SummerCon

20th September 2019

Problem Statement

The Mekong River originates in the Tibetan Plateau and flows through China, Myanmar, Laos, Thailand, Cambodia, and Vietnam. Its upper portion, the Lancang River, has abundant hydropower potential, which has been largely exploited during the three recent decades.

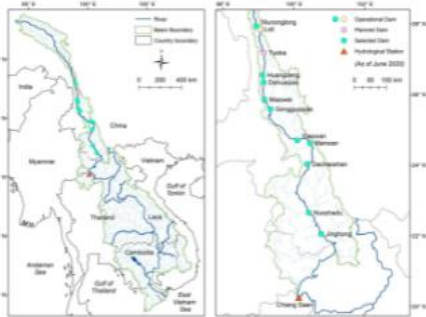


Figure 1. Mekong river basin (left) and location of hydropower dams in the Upper Mekong basin (right)

To date, there are 10 large dams (volume larger than 100 MCM) in the Lancang, controlling about 40% of the annual flow at Chiang Saen (the most upstream station of the Lower Mekong).

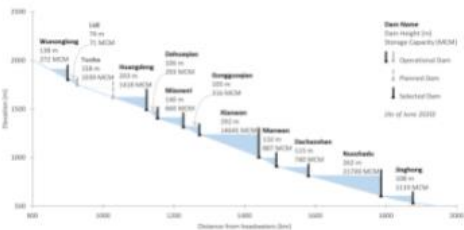


Figure 2. Cascade reservoirs system in the Upper Mekong basin

The amount of water withheld in these dams is a potential source of controversy between China and

Methodology

To overcome this challenge, we exploit satellite images (Landsat) and altimetry data (Jason 2 and 3). The analysis focuses on 10 reservoirs and is conducted in three steps (figure 3).

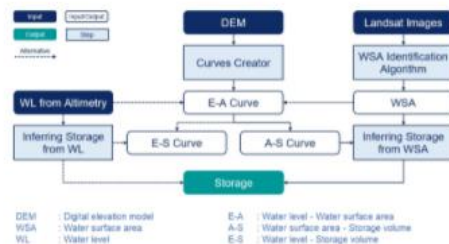
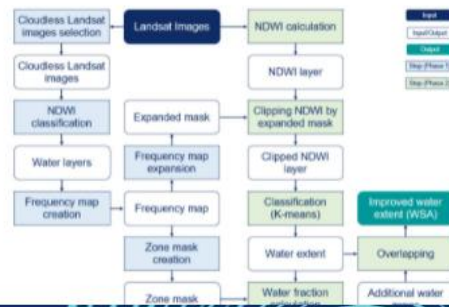


Figure 3. Methodology framework

1. Create the E-A curve for each reservoir by using DEM data (or pairing satellite-image-derived WSA with altimetry-derived water level). Convert each E-A curve into A-S and E-S curves.
2. Calculate WSA from satellite images. In this step, we apply the WSA identification algorithm (figure 4) to solve misclassification due to clouds and shadow on the Landsat images.
3. Derive reservoirs' storage from calculated WSA or altimetry-derived water level by using A-S and E-S curves.



Result (1)

E-A, A-S, and E-S Curves

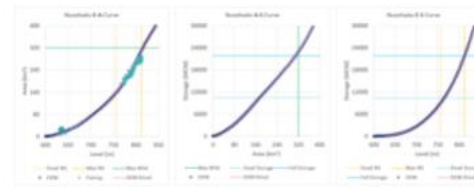


Figure 5. E-A, A-S, and E-S curves of Nuozhadu reservoir

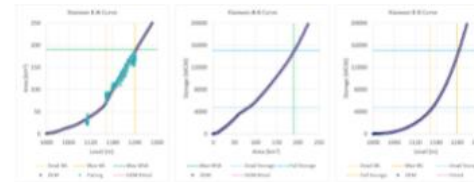


Figure 6. E-A, A-S, and E-S curves of Xiaowan reservoir

Remote-sensing-derived Water Surface Area

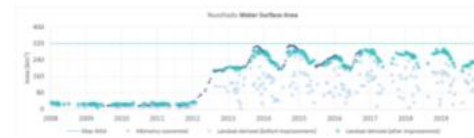


Figure 7. Nuozhadu reservoir's water surface area

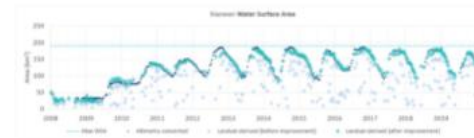


Figure 8. Xiaowan reservoir's water surface area

Result (2)

Storage Variation

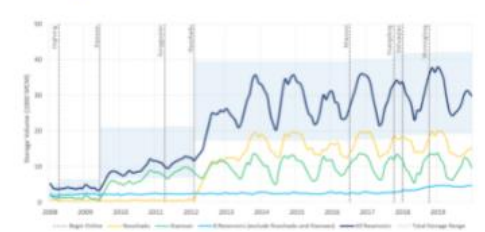


Figure 9. Storage variation in the Upper Mekong's reservoirs (Manwan and Dachaoshan began online in 1992 and 2003 respectively)

Reservoirs' Storage and Downstream Discharge

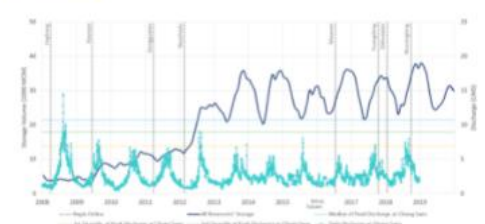
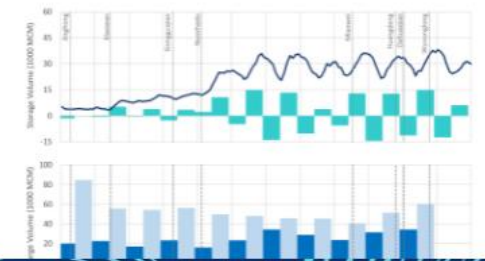


Figure 10. Upper Mekong reservoirs' storage and discharge at Chiang Saen station (data source: Mekong River Commission)



Dung Trung Vu, Thanh Duc Dang, and Stefano Galelli

Pillar of Engineering Systems and Design, Singapore University of Technology and Design

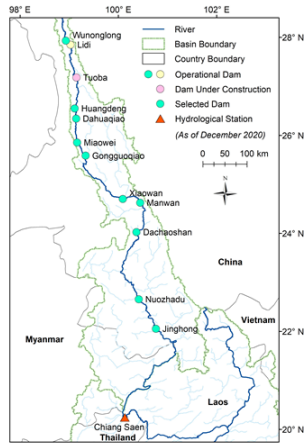


Figure 1. Location of the dams on the Lancang River

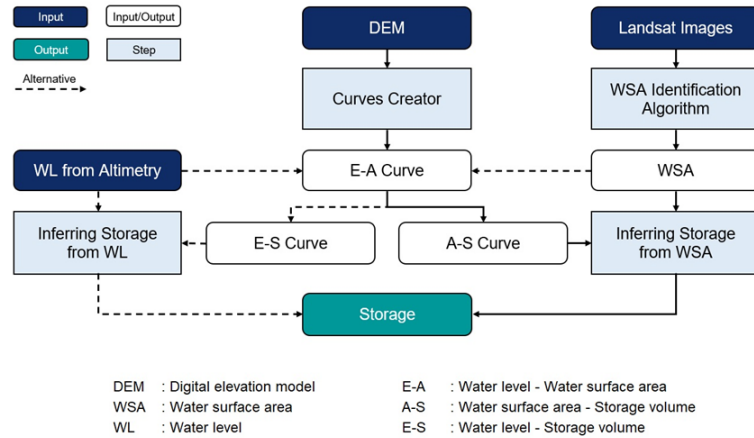


Figure 3. Methodological framework

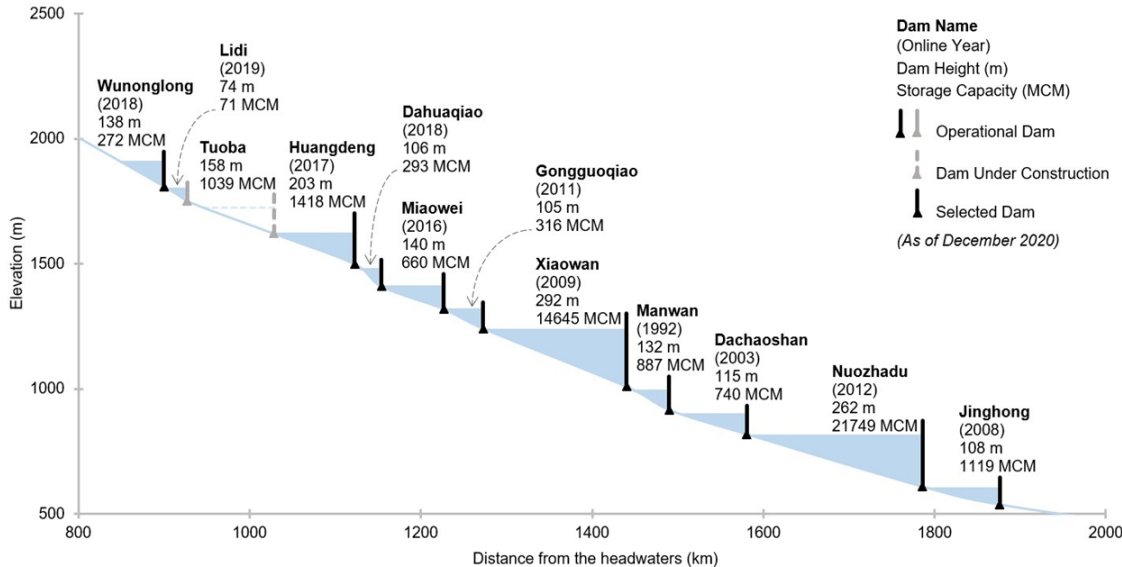


Figure 2. Cascade reservoirs system on the Lancang River

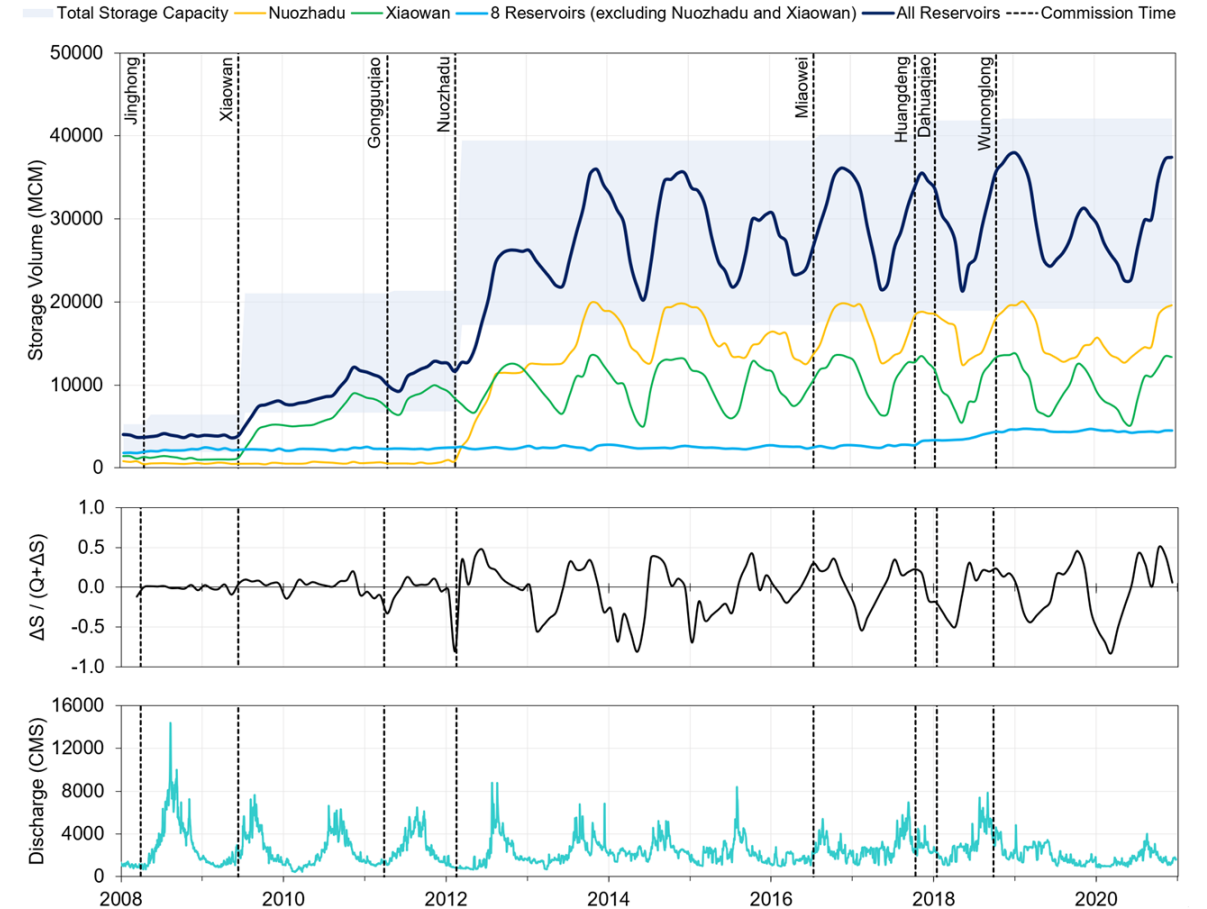


Figure 4. Storage variation of Lancang reservoirs and storage variation range of the whole system (top), ratio of the change in storage volume of the reservoir system (ΔS) to the sum of discharge volume at Chiang Saen and the change in storage volume of the reservoir system ($Q + \Delta S$) (middle), and daily discharge at at Chiang Saen (source: MCR) (bottom).